MAX-PLANCK-INSTITUT
FÜR PLASMAPHYSIK

The effect of geometry and profiles on turbulent electron transport in W7-X

G.M. Weir, J.-P. Bähner, H. Trimiño-Mora, O. Grulke, T. Stange,
E. Maragkoudakis, A. Krämer-Flecken, J. Arnaiz-Guerrero,
S. Bozhenkov, K.J. Brunner, G. Fuchert, J. Geiger, M. Hirsch,
J. Knauer, A. Langenberg, V. Murugesan, N. Pablant, E. Pasch,
T. Schröder, A .v. Stechow, H.M. Smith, J. Wagner, M. Zimmermann,
T. Klinger and the W7-X Team

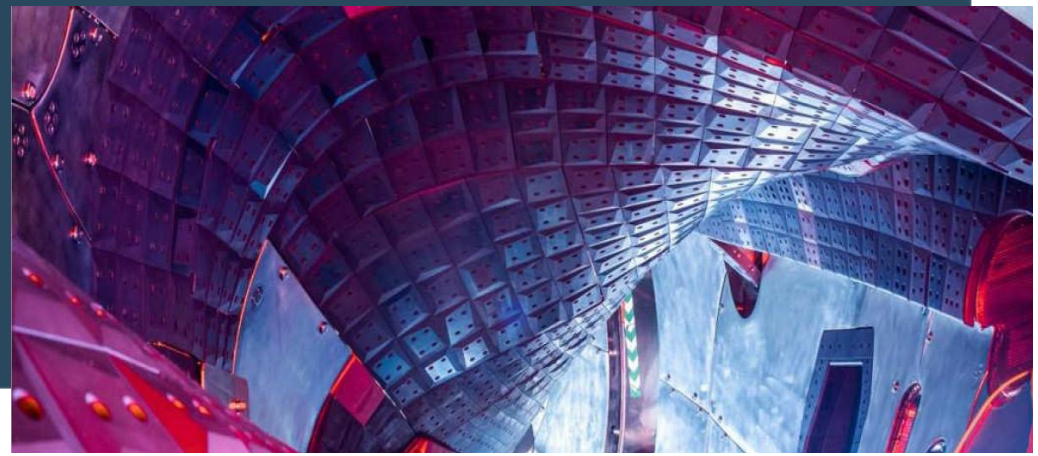

EUROfusion

This work has been carried out within the framework of the EUROfusion Consortium, funded by the European Union via the Euratom Research and Training Programme (Grant Agreement No 101052200 — EUROfusion). Views and opinions expressed are however those of the author(s) only and do not necessarily reflect those of the European Union or the European Commission. Neither the European Union nor the European Commission can be held responsible for them.

Wendelstein 7-X – operation parameters

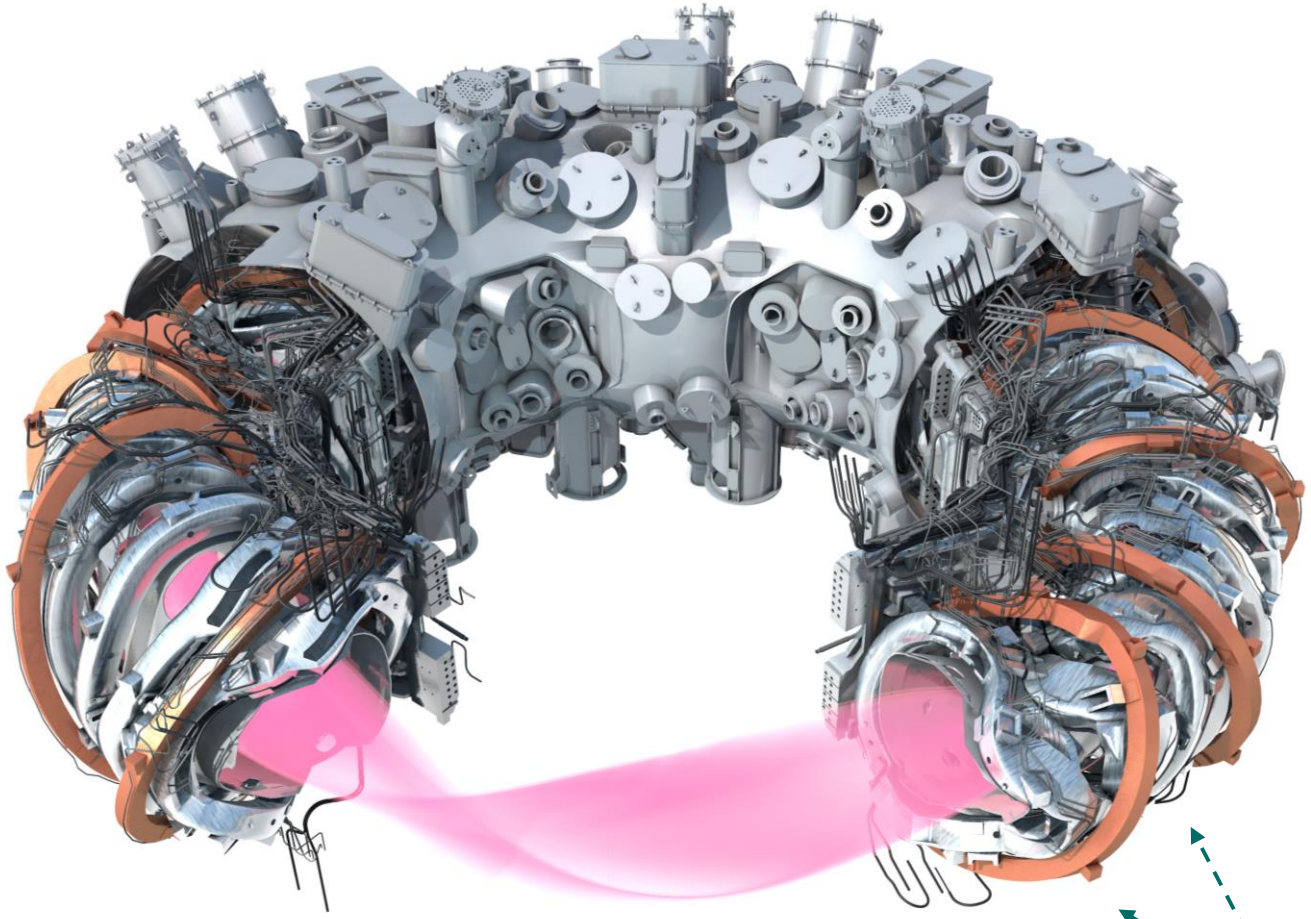

50 non-planar / 20 planar superconducting coils

quantity	Unit	value
magnetic induction	T	2.5
ECRH power	MW	8.5
NBI power	MW	6 (>10)
neutral gas		H_2, He (D_2)
Major / minor radius	m	5.5 / 0.5
plasma volume	m^3	30
typical pulse length	s	≤30 (1800)
rotational transform	2π	5/6 … 5/4

As rotational transform is varied, so does the edge divertor solution

M. Kriete – Wed./9:00 – *How scrape-off layer drift effects change with magnetic field strength in W7-X*

S. Thiede – Wed./9:30 – *Analysis of the 3D heat fluxes in the island divertor of W7-X*

A. Kharwandikar – Thurs./ 9:30 – *Empirical scaling of heat transport tin the W7-X Island Divertor*

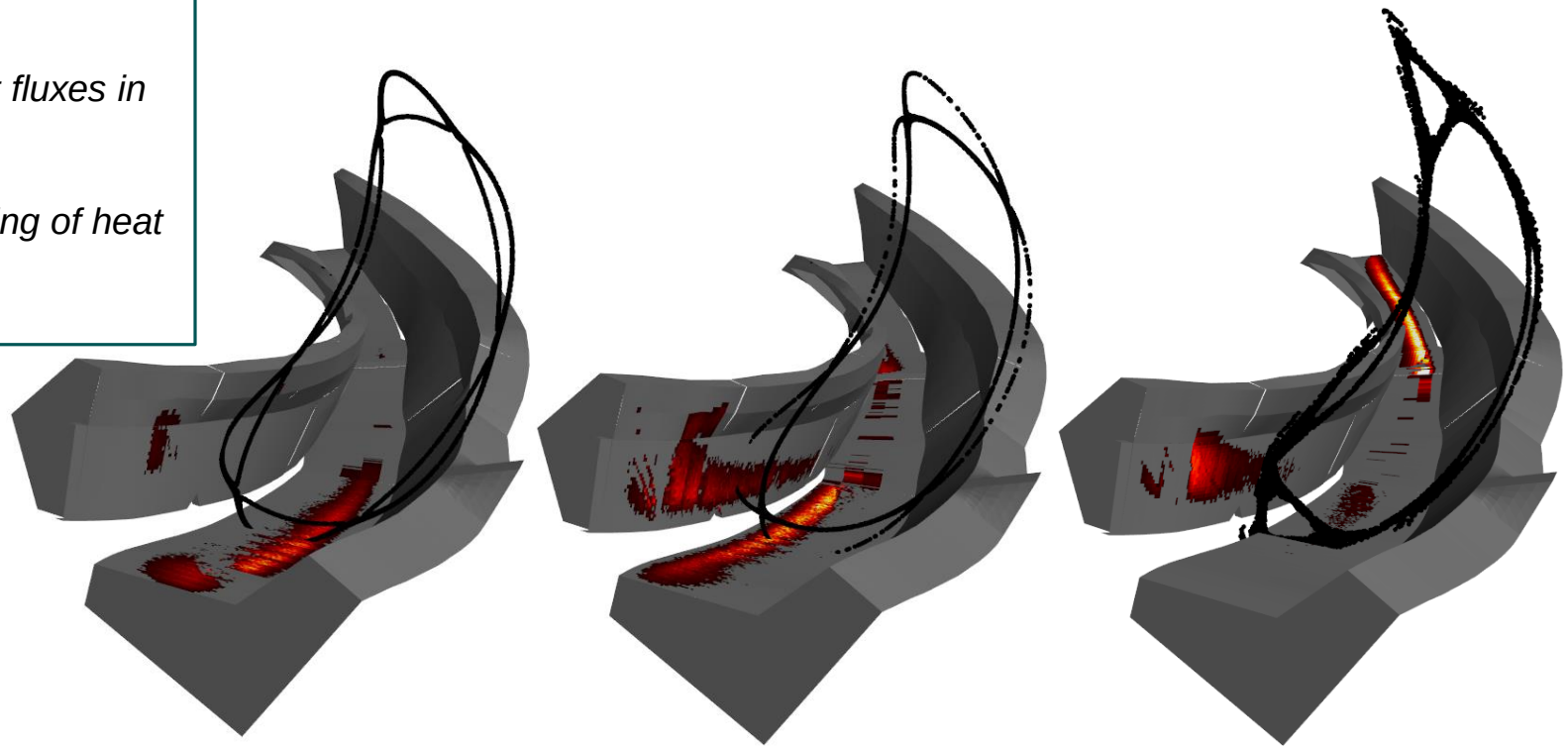

mirror ratio -0.005 … 0.32

iota at magnetic axis 0.72 – 1.07

radial shift : difference in planar coils A/B

„low iota“ $\iota = {}^{5}/_{6}$

0.54 m / 31.9 m³

„standard“ $\iota = {}^{5}/_{5}$

0.51 m / 28.6 m³

„high iota“ $\iota = {}^{5}/_{4}$

0.50 m / 26.7 m³

Divertor images courtesy: V., Winters

As rotational transform is varied, so does the edge divertor solution

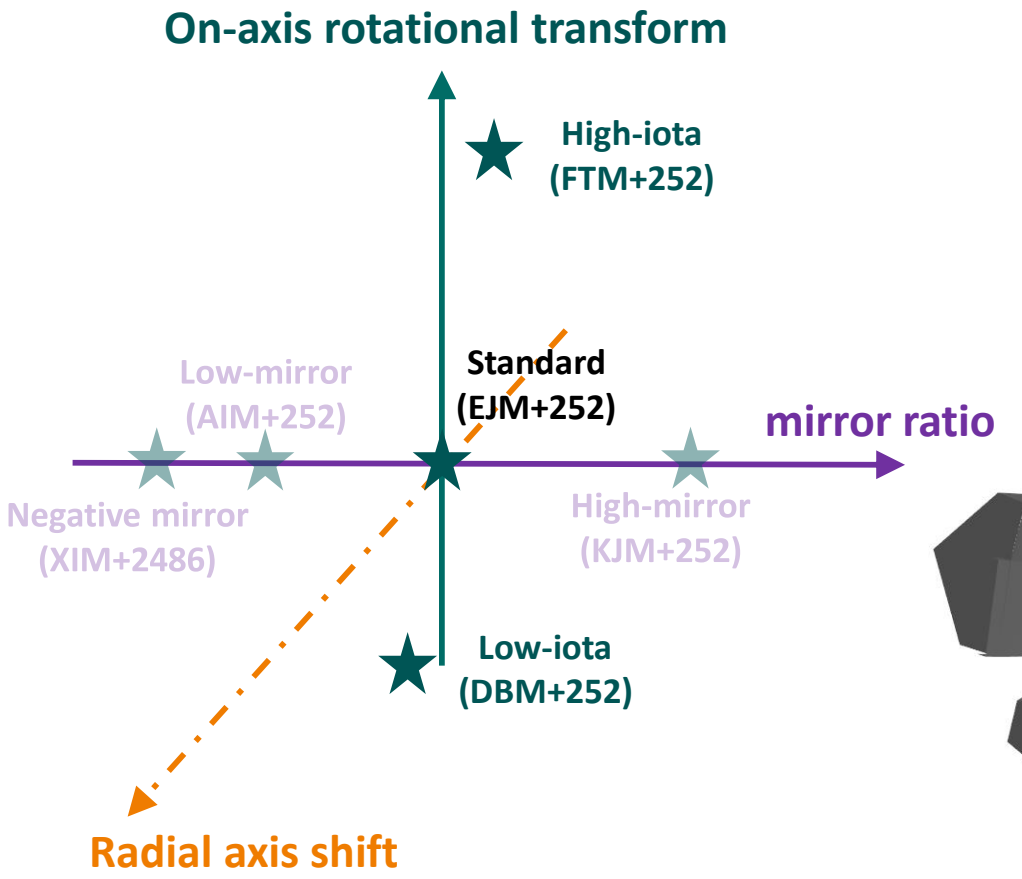

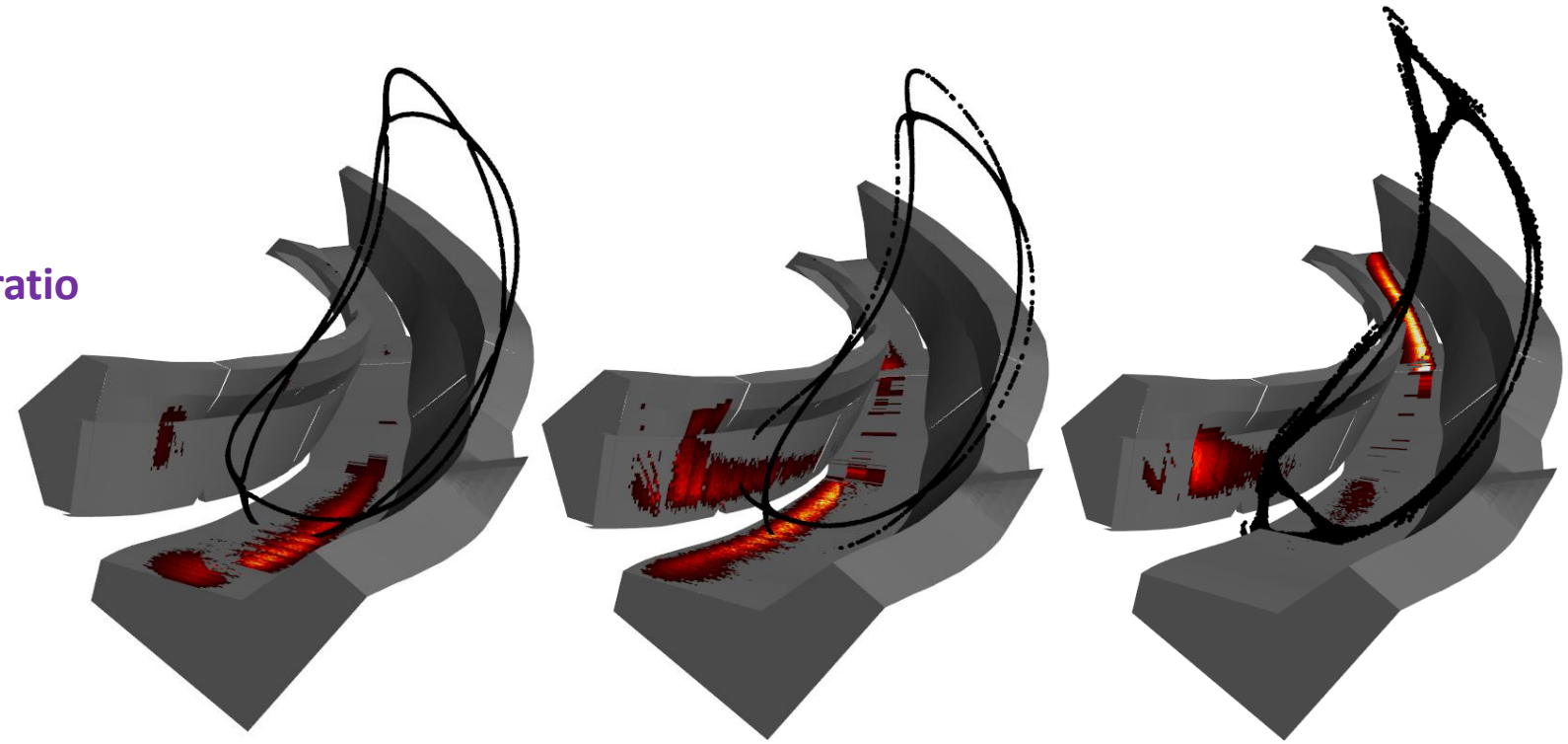

„low iota“ $\iota = {}^{5}/_{6}$

„standard“ $\iota = {}^{5}/_{5}$

„high iota“ $\iota = {}^{5}/_{4}$

mirror ratio -0.005 … 0.32

iota at magnetic axis 0.72 – 1.07

radial shift : difference in planar coils A/B

0.54 m / 31.9 m³

0.51 m / 28.6 m³

0.50 m / 26.7 m³

Divertor images courtesy: V., Winters

Core electron heat transport is characterized through power balance and heat pulse propagation experiments on W7-X

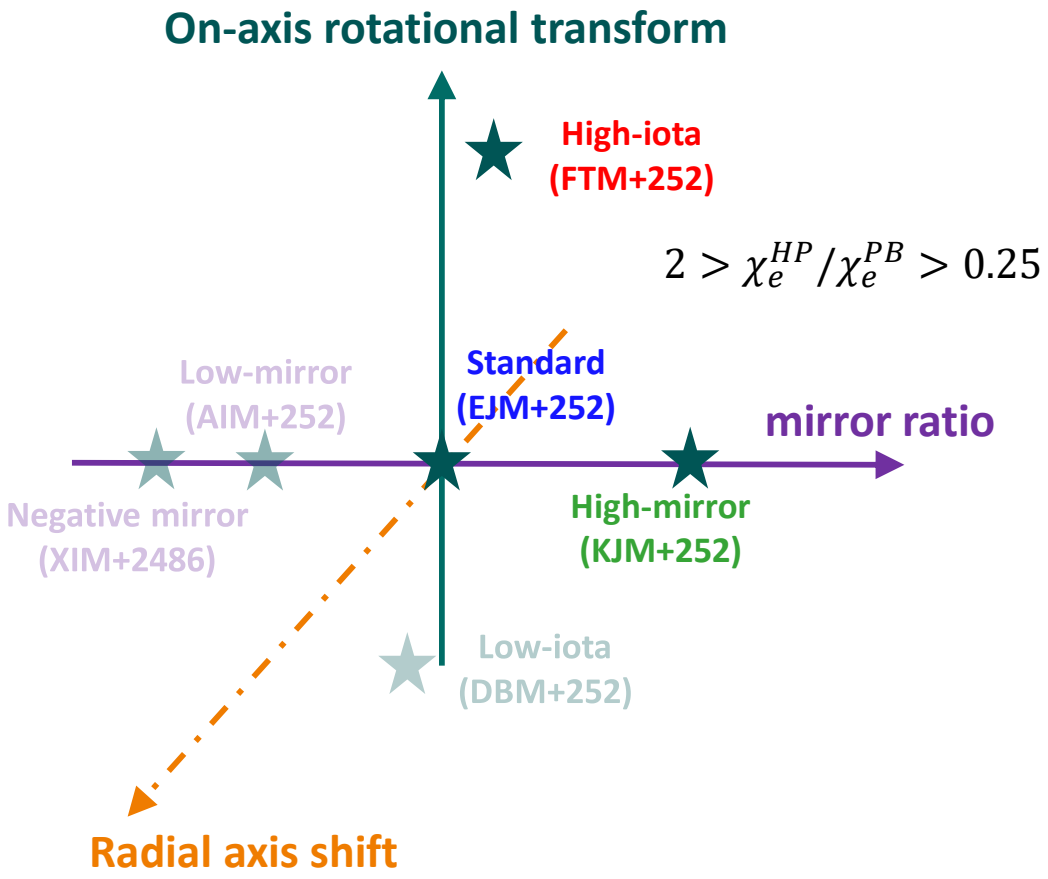

mirror ratio -0.005 … 0.32

iota at magnetic axis 0.72 – 1.07

radial shift : difference in planar coils A/B

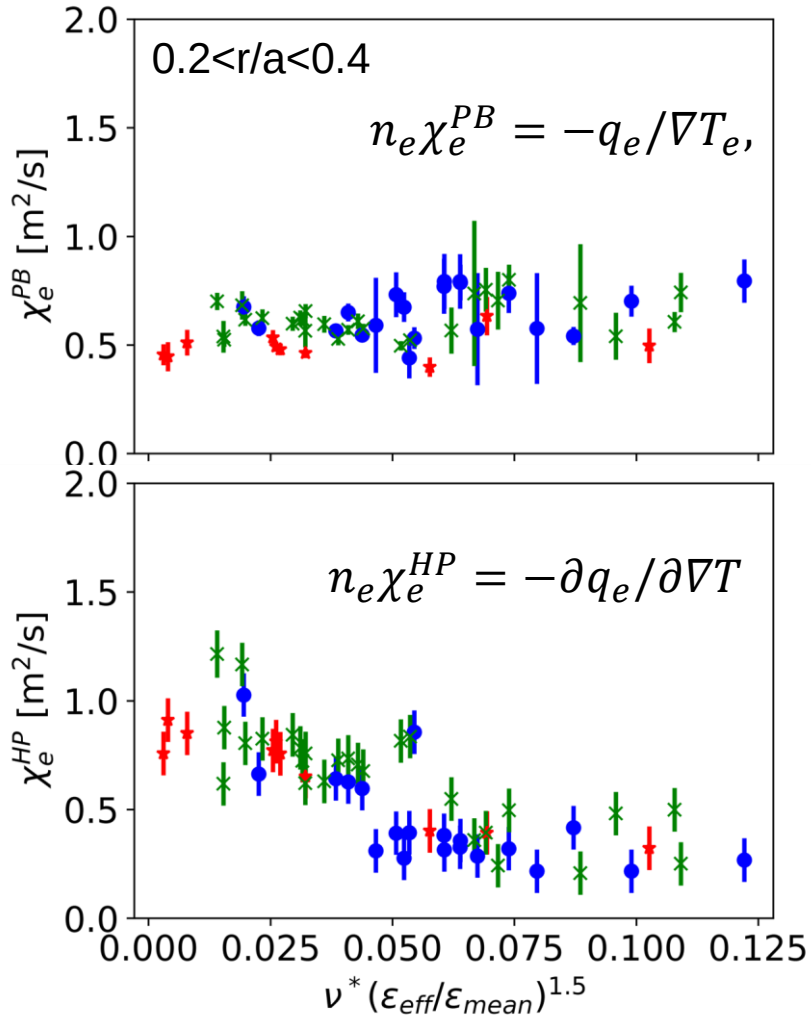

High-iota
Standard
High-mirror

G.M. Weir, P. Xanthopoulos, M. Hirsch et. al NF 61 (2021)

Magnetic configurations discussed here lie on the iota-mirror plane

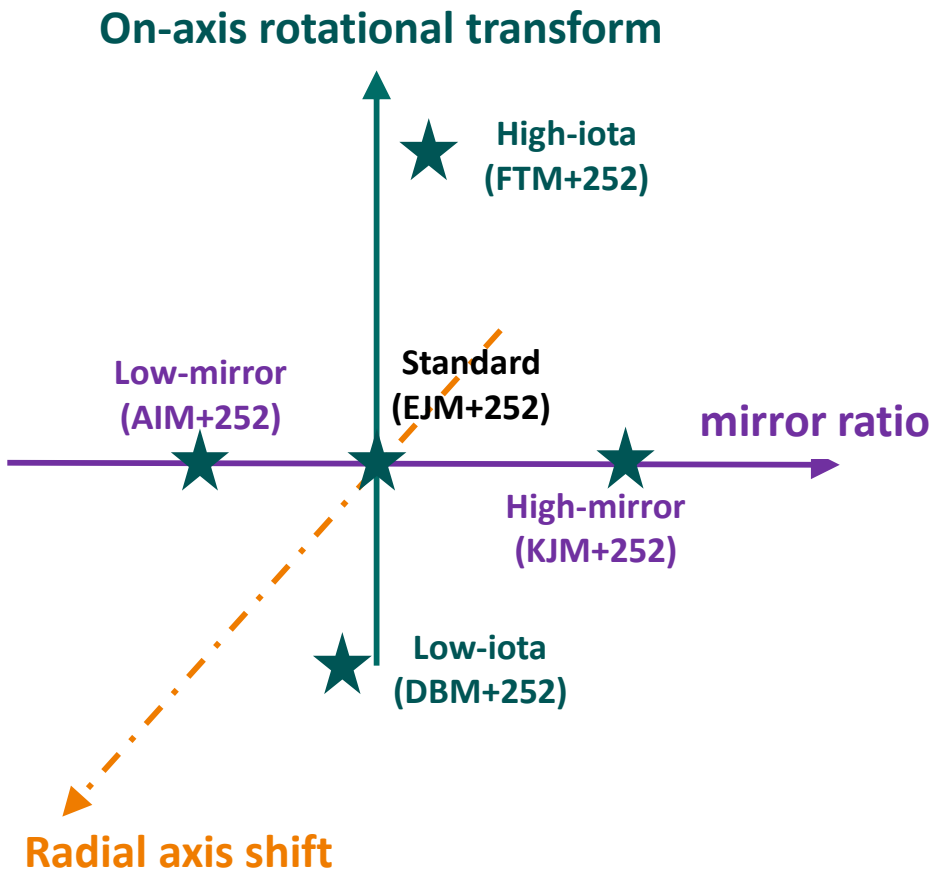

<u>OP2.1 "Umbrella" format</u>:

equilibration (1s)

Flat-top phase (1s)

ECRH modulation (1.5s)

Perturbative phase (0.5s)

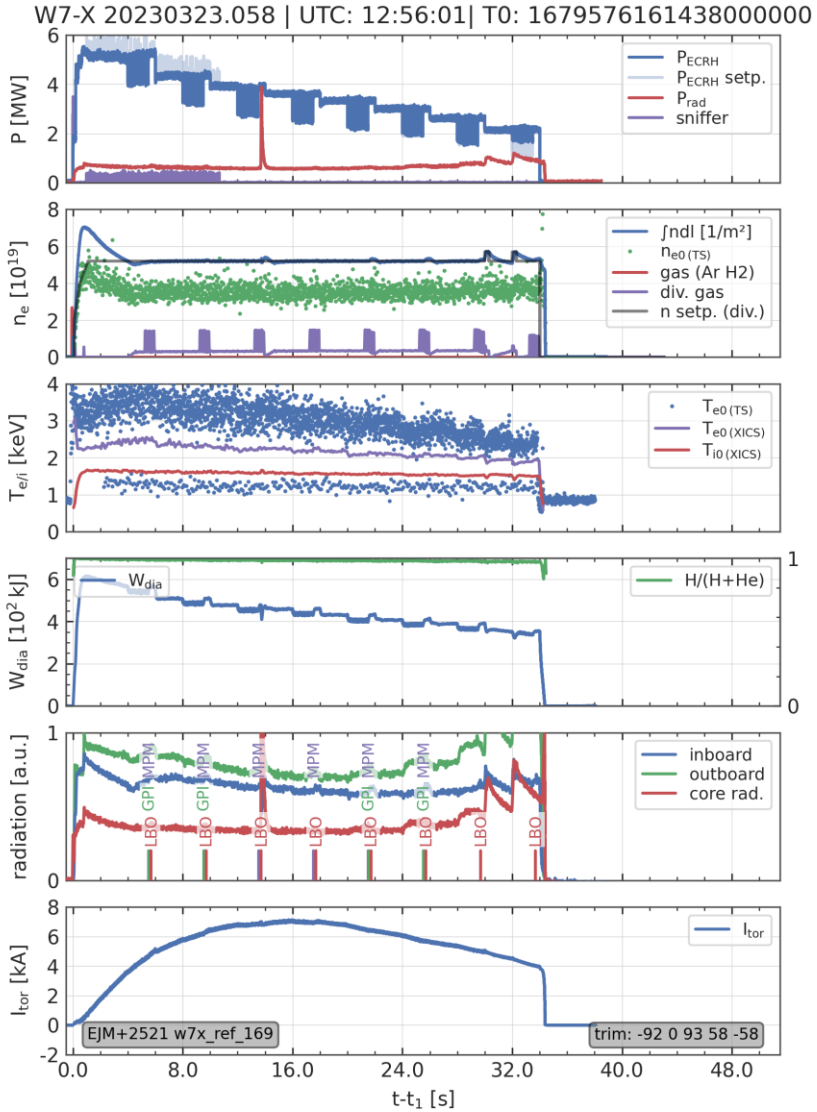

The Phase Contrast Imaging (PCI) diagnostic measures a significant increase in fluctuation magnitude at low-iota

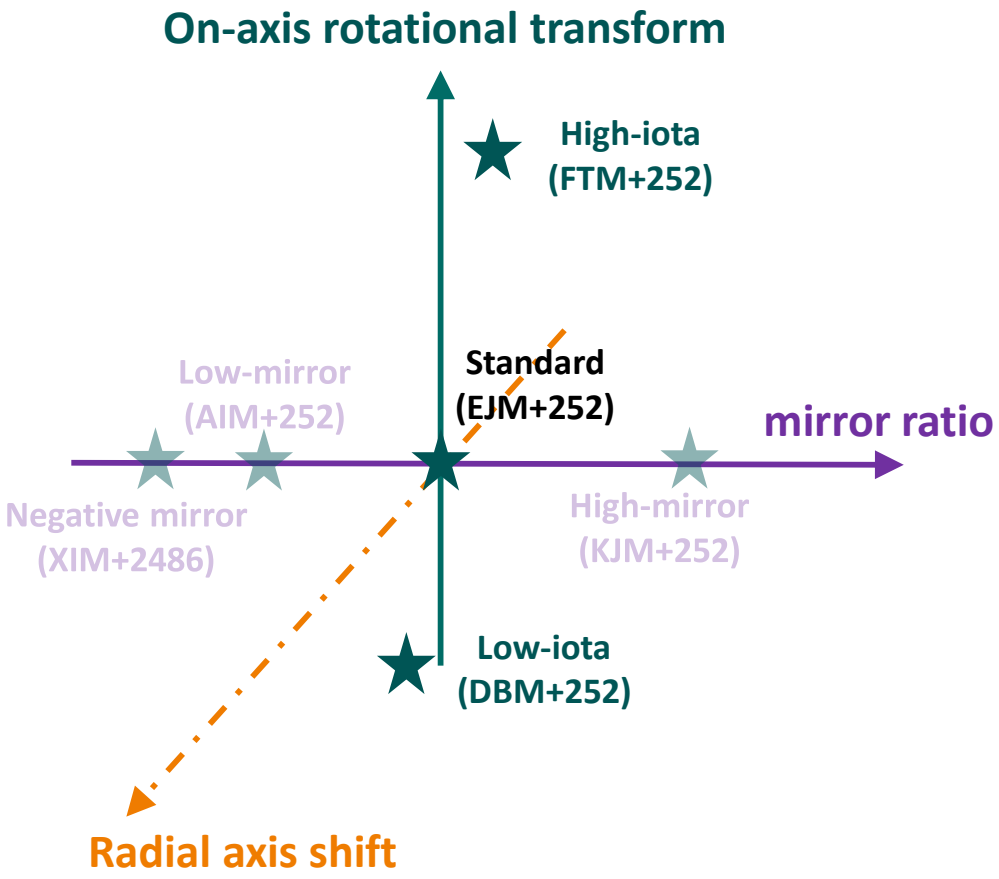

mirror ratio -0.005 … 0.32

iota at magnetic axis 0.72 – 1.07

radial shift : difference in planar coils A/B

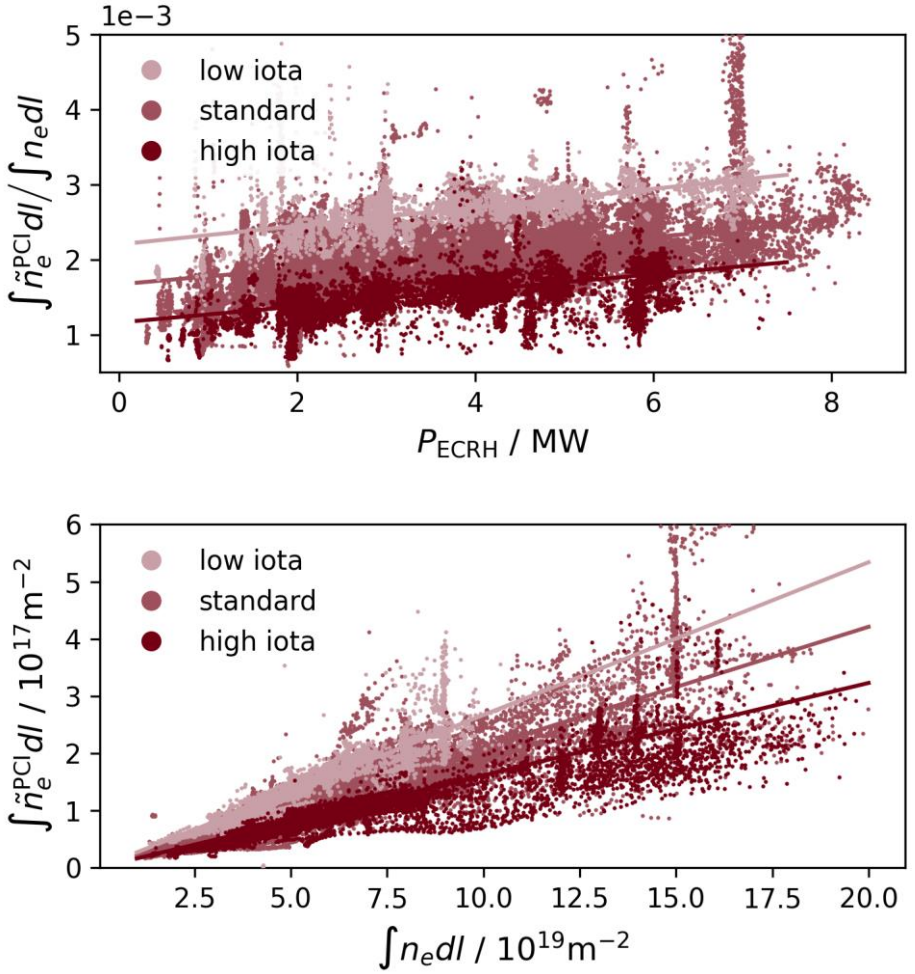

J.-P. Bähner, L. Podavini, A. Bañón Navarro et. al NF 66 (2026)

As mirror ratio varies, so does the degree of neoclassical optimization (quasi-isodynamicity with a maximum in on-axis *J*)

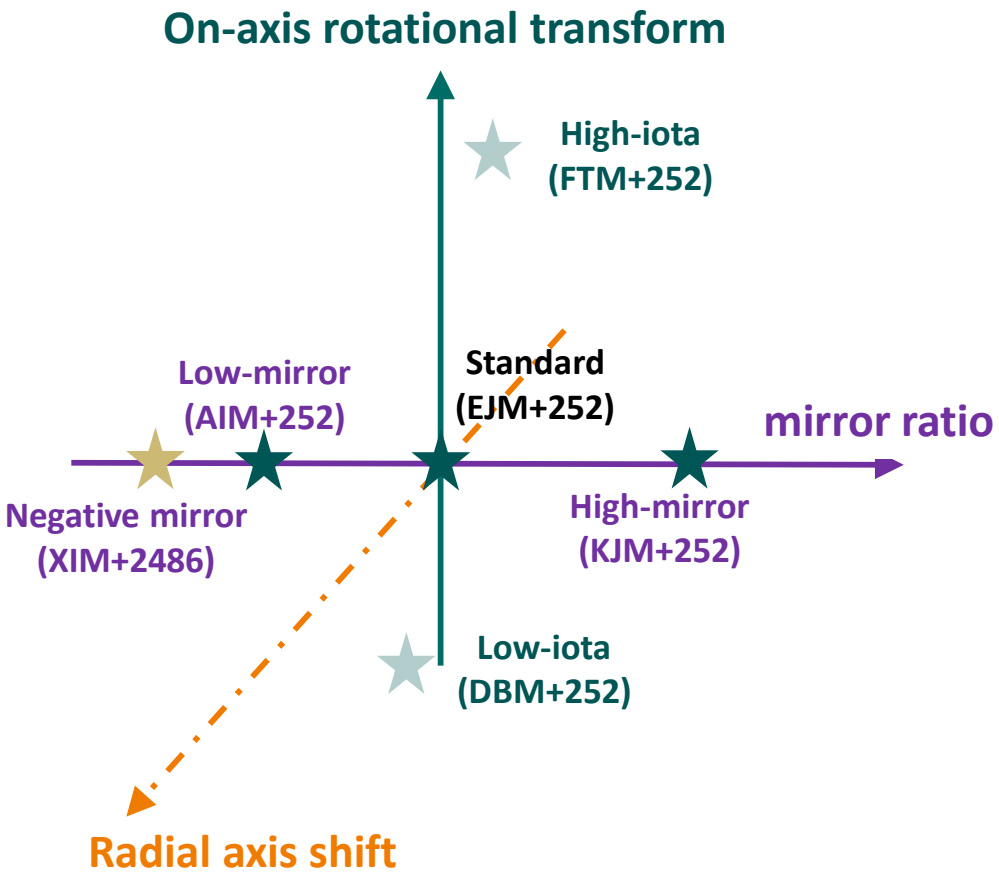

mirror ratio -0.005 … 0.32

iota at magnetic axis 0.72 – 1.07

radial shift : difference in planar coils A/B

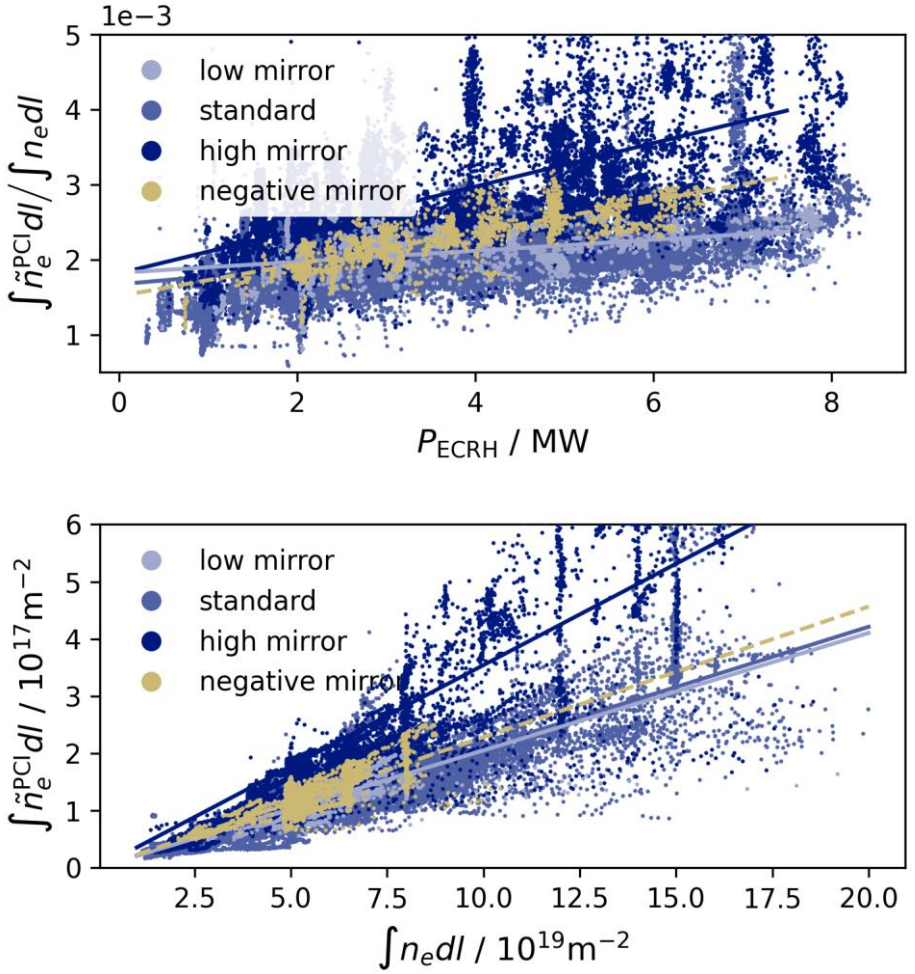

J.-P. Bähner, L. Podavini, A. Bañón Navarro et. al NF 66 (2026)

A Quasi-coherent mode (QCM) has been observed in the outer half-radius of the standard configuration

QCM – a mode that develops bandwidth through interaction with the background turbulence

Poloidal correlation reflectometry (PCR) measures a broad coherent mode : ~200-400 kHz range

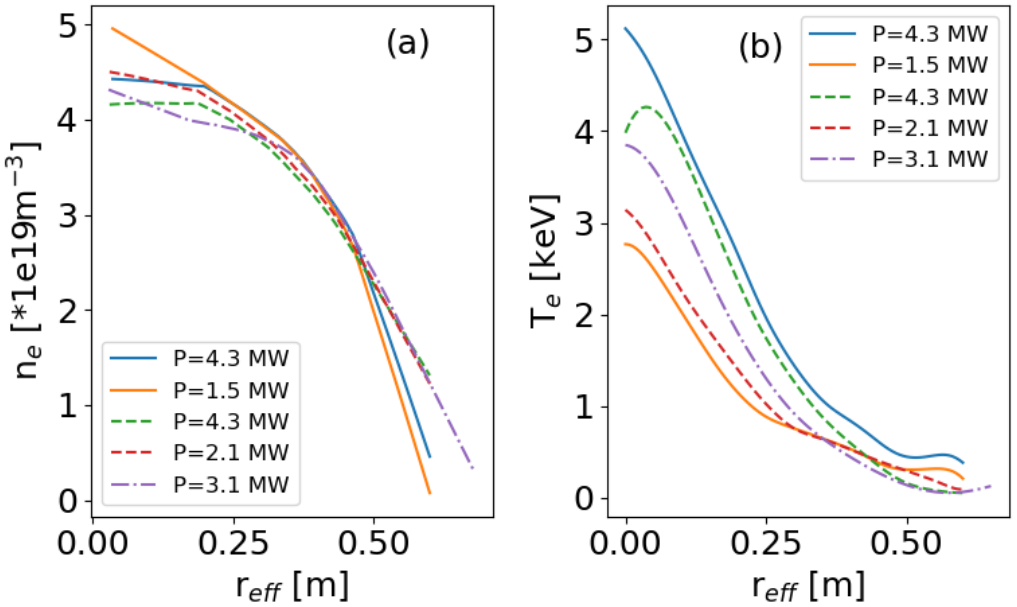

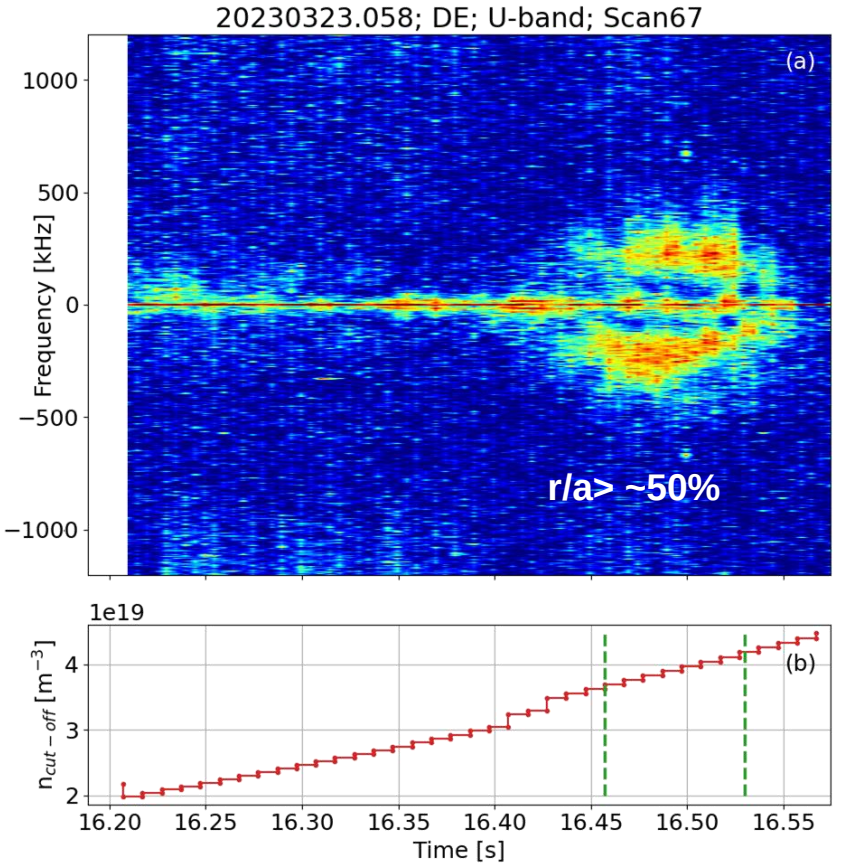

→ ***PCR limited to <4.5x10^{19} m^{-3} in OP2.1-3***

A. Krämer-Flecken, J. Proll, G.M. Weir, et. al PPCF 67 (2025)

This QCM also generates significant electron temperature fluctuations in the outer half-radius

The Correlation ECE diagnostic can measure across the plasma minor radius

→ measures T_e fluctuations embedded in the blackbody emission

→ 2025 onwards: includes 16 radially scannable channels

XP:20230323.058 (14.2-16.0 s)

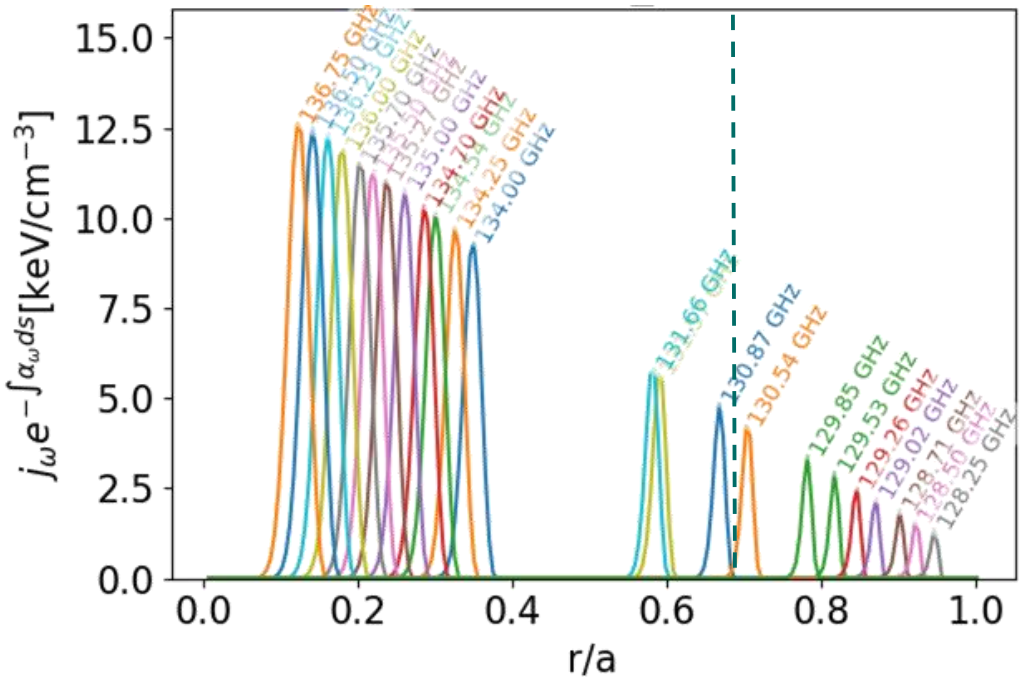

(130.8/130.4 GHz)

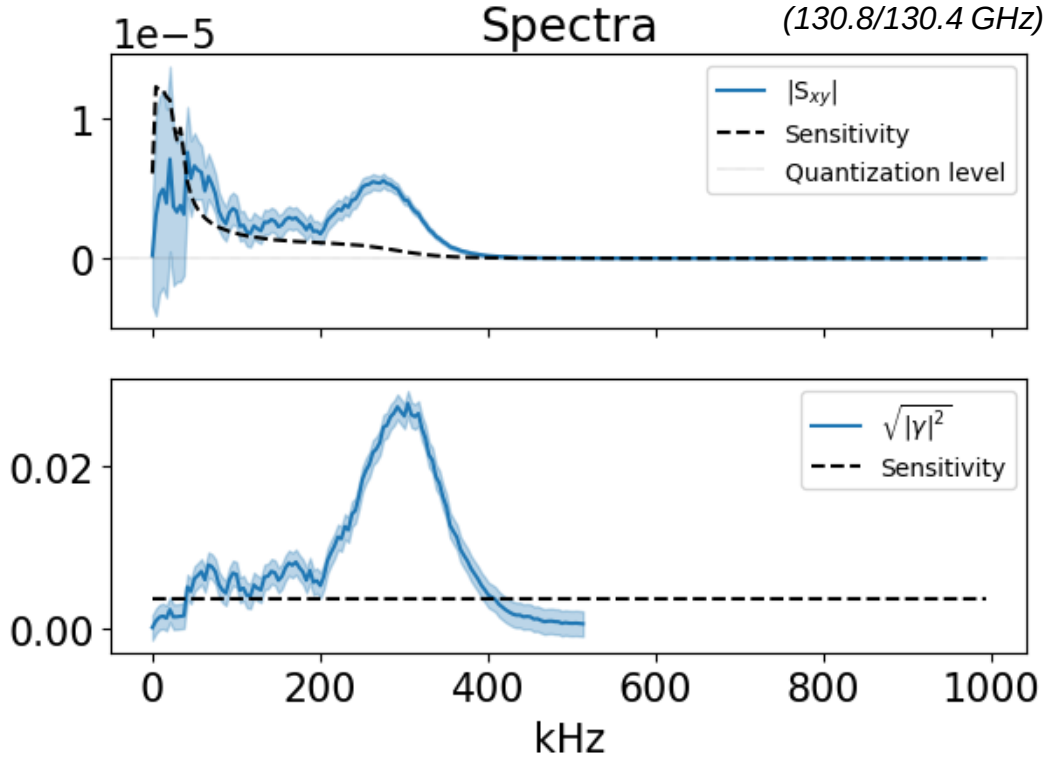

The magnitude of T_e fluctuations increase in the region of the QCM : 60-90% minor radius

The Correlation ECE diagnostic can measure across the plasma minor radius

→ measures T_e fluctuations embedded in the blackbody emission

→ 2025 onwards: includes 16 radially scannable channels

XP:20230323.058 (14.2-16.0 s)

(130.8/130.4 GHz)

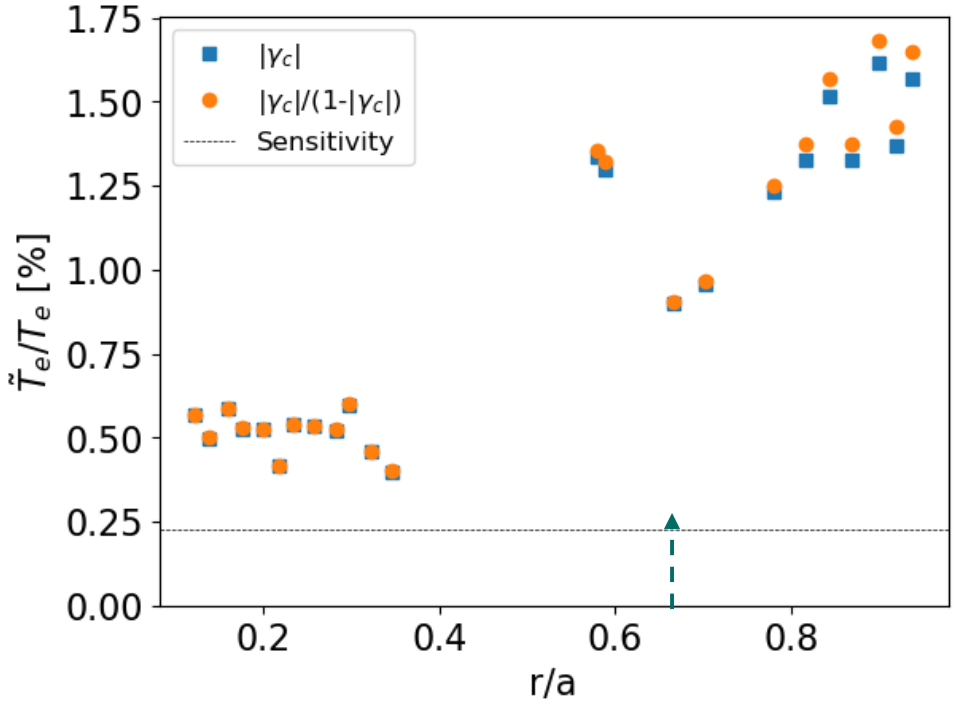

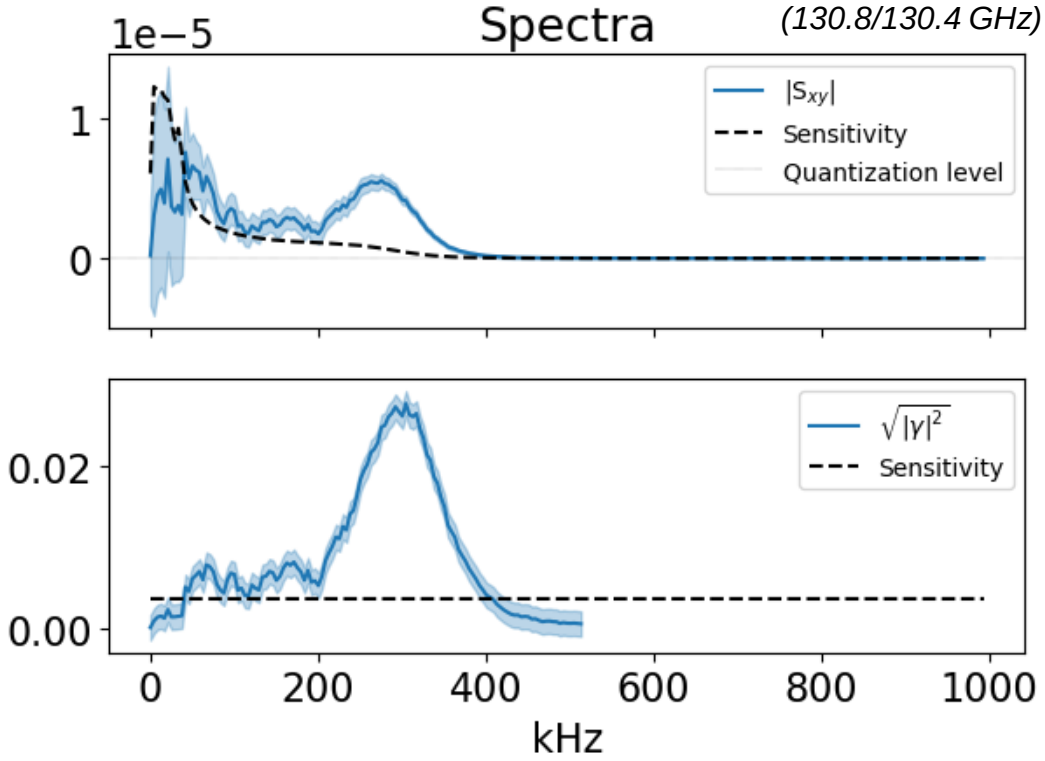

The Quasi-coherent mode (QCM) appears to stabilize in the high-mirror configuration

QCM – a mode that develops bandwidth through interaction with the background turbulence

The QCM rotates in the elec. diamagn. direction and is reduced in the high-mirror configuration;

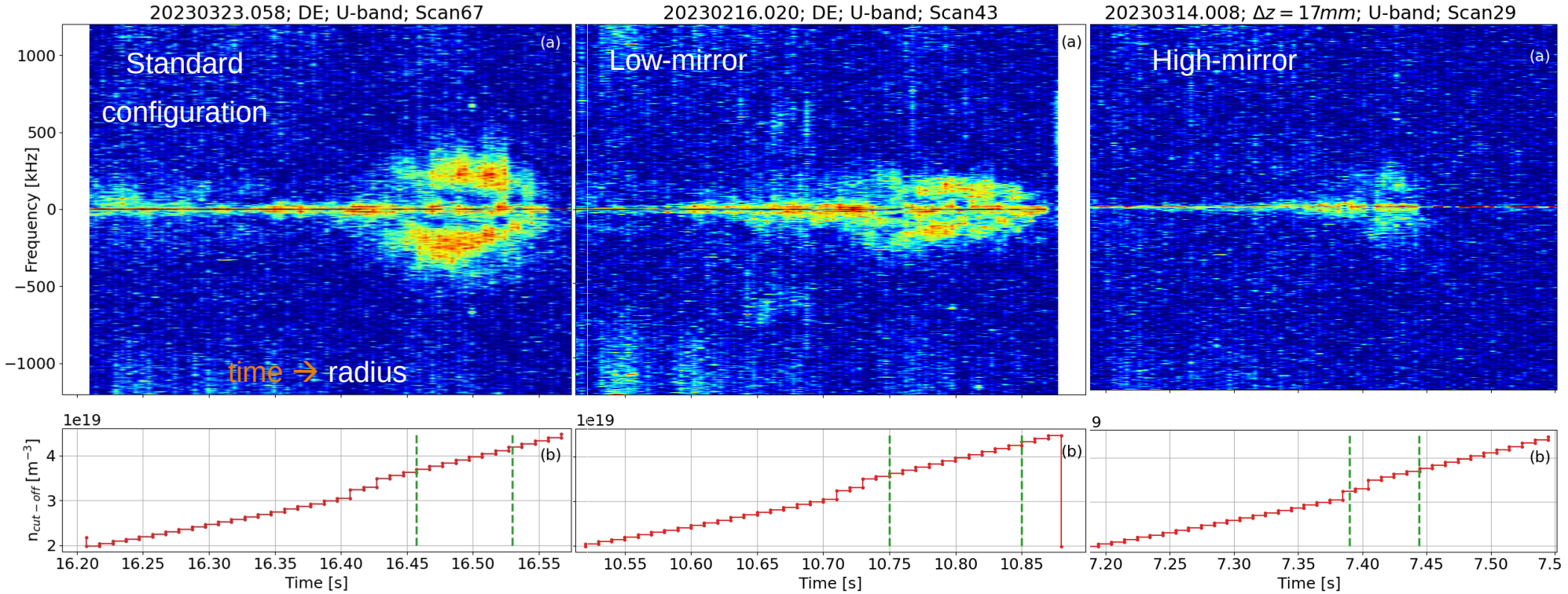

Associated with TEM turbulence

A. Krämer-Flecken, J. Proll, G.M. Weir, et. al PPCF 67 (2025)

Magnetic configuration space discussed here lies on the iota-mirror plane

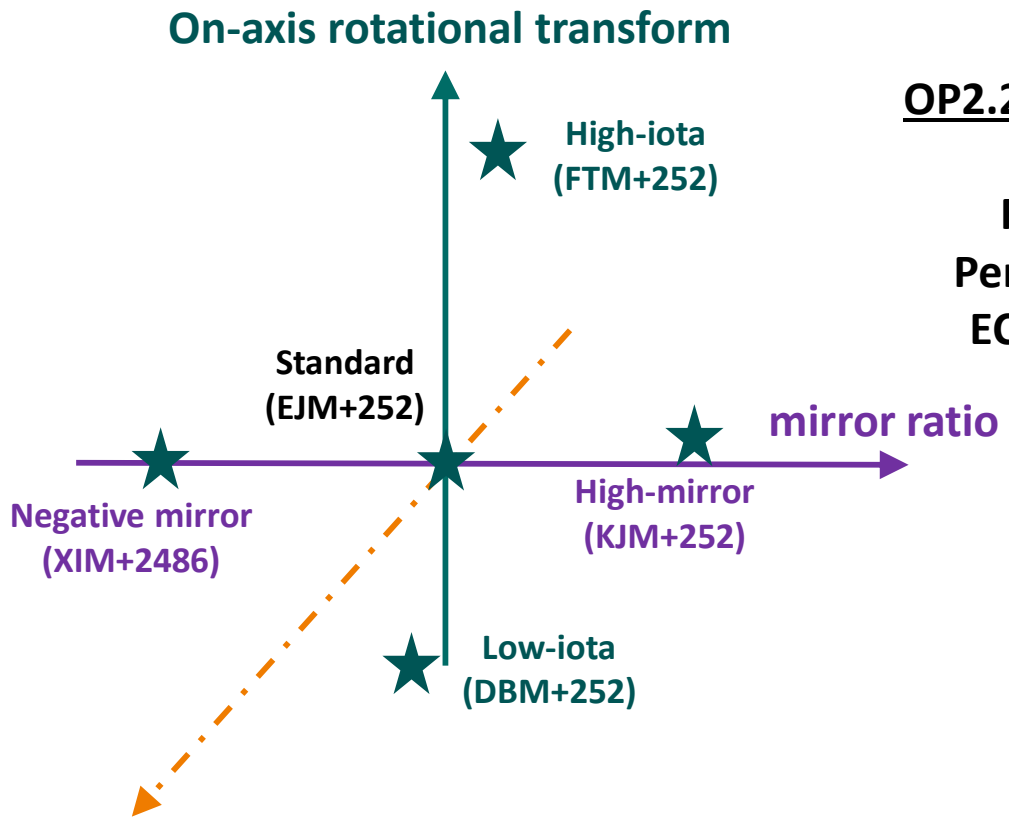

mirror ratio -0.005 … 0.32

iota at magnetic axis 0.72 – 1.07

radial shift : difference in planar coils A/B

OP2.2/3 "Umbrella" format:

equilibration (1s)

Flat-top phase (1s)

Perturbative phase (1s)

ECRH modulation (1s)

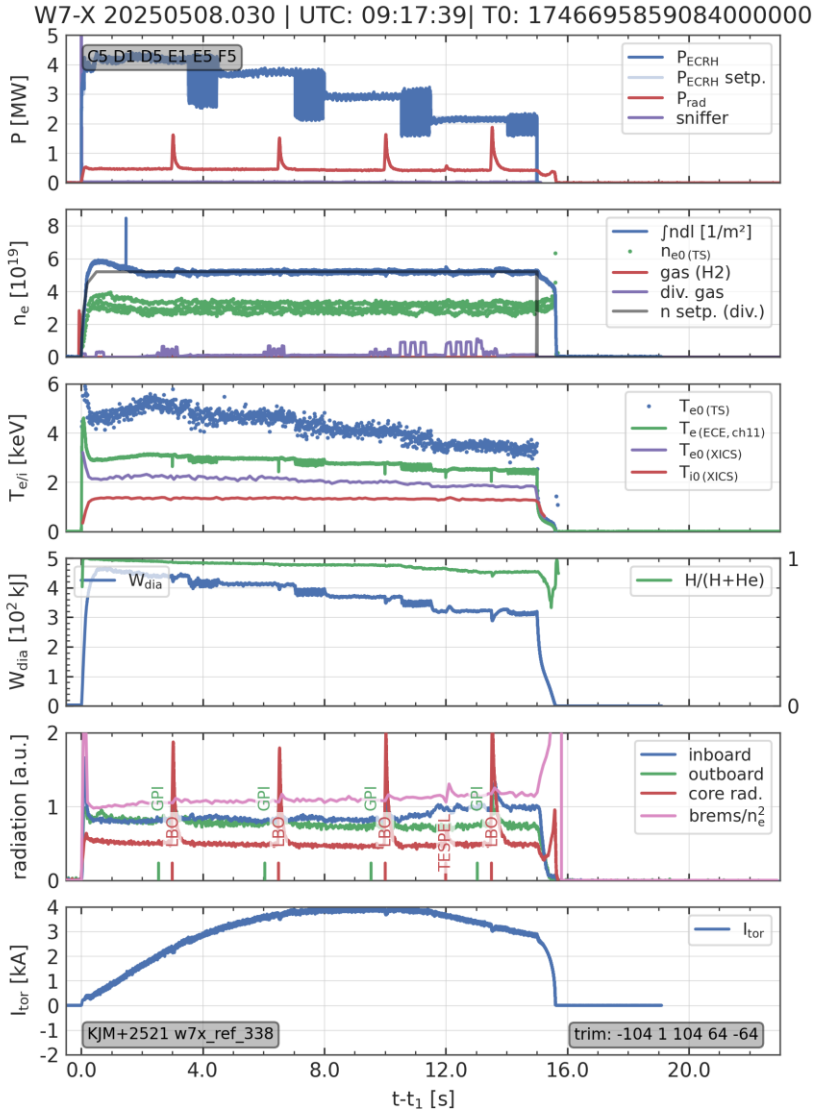

Heat transport in W7-X is characterized through power balance analysis and heat pulse propagation experiments

Power balance analysis: 4.2MW ECRH / [1.0 – 4.5 s]

Thomson scattering: n_e, T_e,

X-ray imaging crystal spectroscopy (XICS): T_i, E_r

Neotransp + DKES : Neoclassical transport

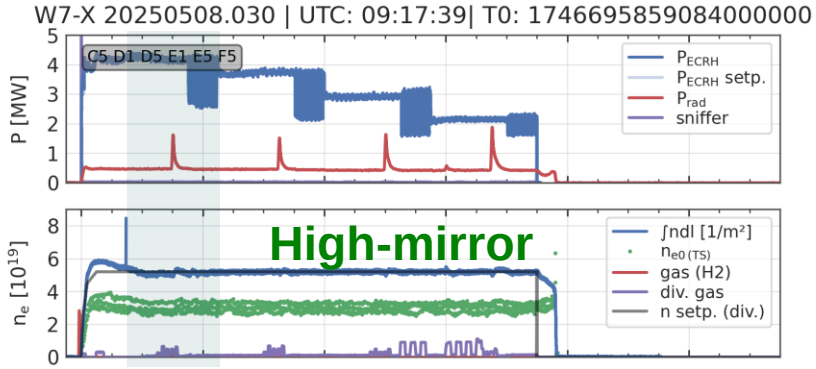

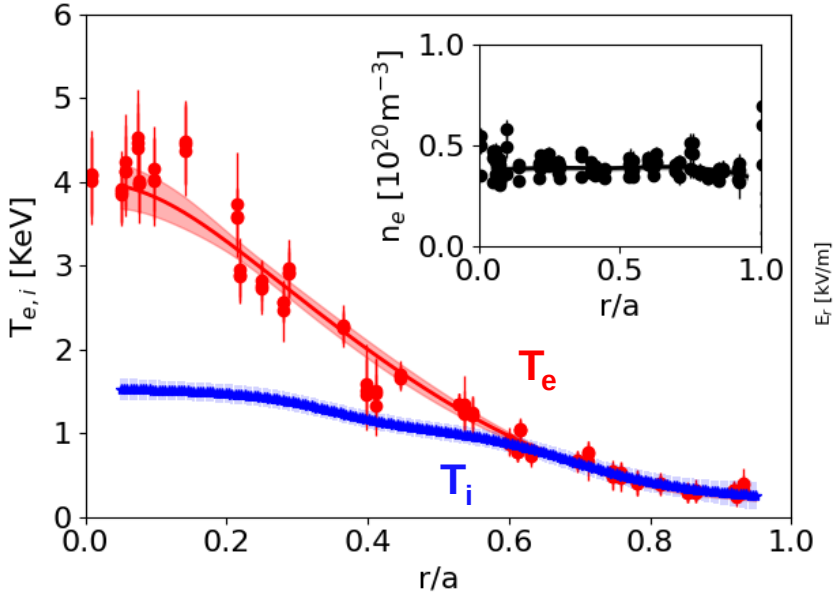

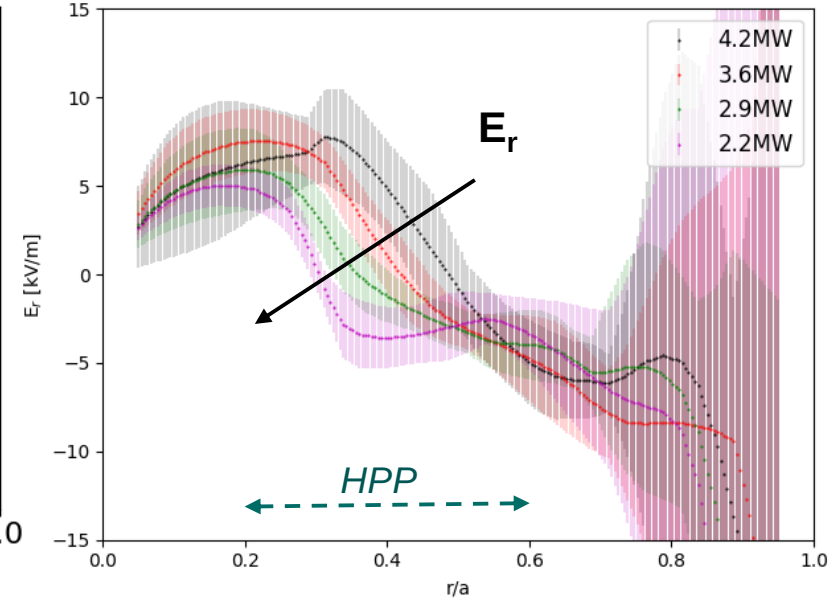

Neoclassical electron heat transport can be significant in the core, but is often low for r/a>50% where anomalous sources dominate

Power balance analysis: 4.2MW ECRH / [1.0 – 4.5 s]

Thomson scattering: n_e, T_e

X-ray imaging crystal spectroscopy (XICS): T_i, E_r

Neotransp + DKES : Neoclassical transport

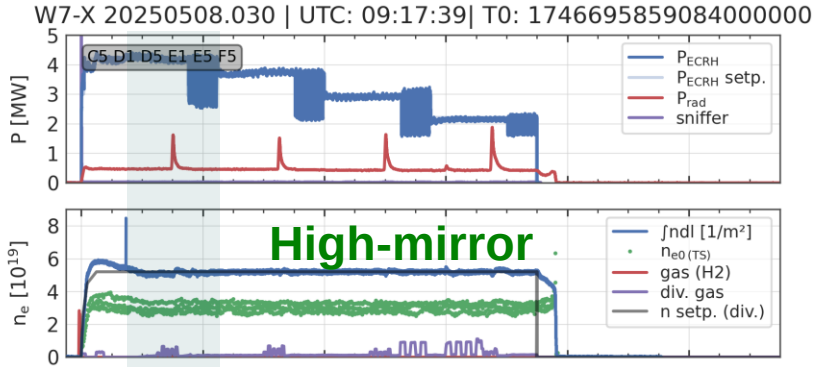

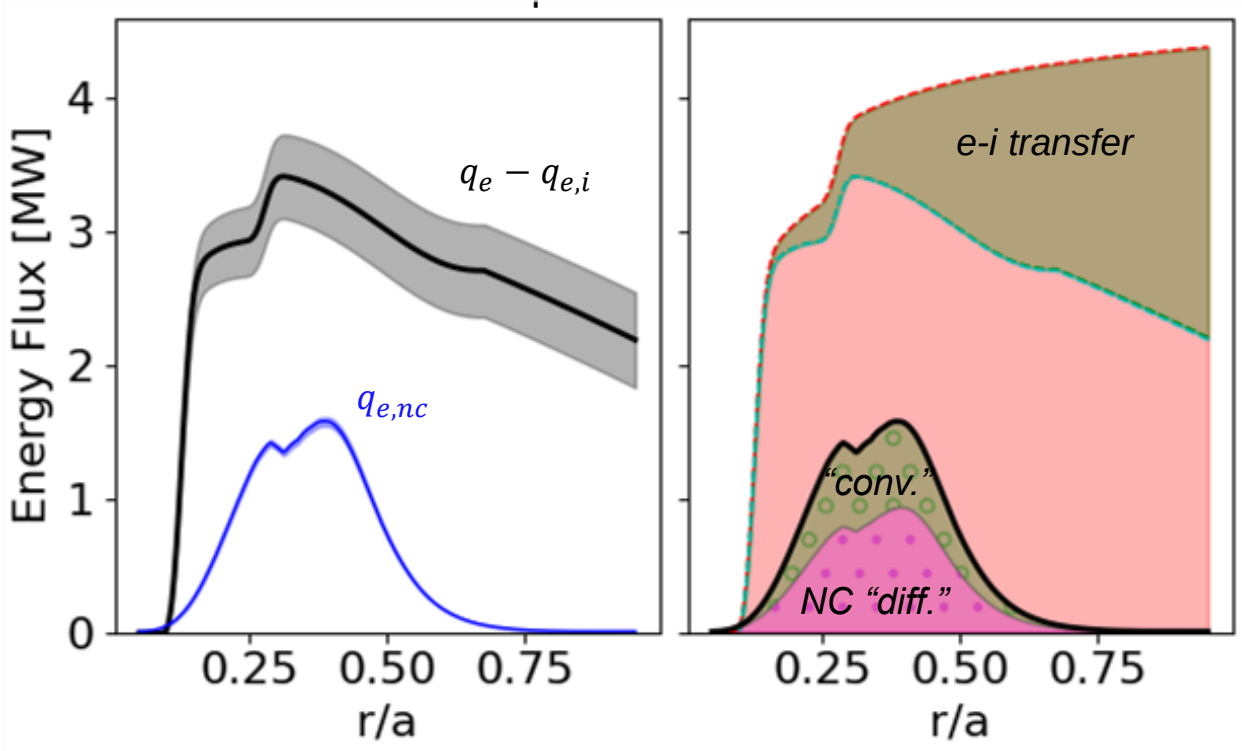

Both the heat pulse and power balance diffusivities decrease as heating power increases

Heat pulse propagation across the electron-ion root transition region yields a stiffness of the order 1:

$$n_e\chi_e^{PB} = -q_e/\nabla T_e, \qquad n_e\chi_e^{HP} = -\partial q_e/\partial \nabla T$$

High-mirror

(0.2<r/a<0.6)	χ_e^{PB} [m²/s]	χ_e^{HP} [m²/s]	dlnT$_e$/dρ	dlnT$_i$/dρ
KJM (4.2MW)	0.61±0.37	0.81±0.08	3.1±0.6	1.2±0.1
KJM (3.6MW)	0.56±0.36	0.68±0.08	3.3±0.6	1.3±0.1
KJM (2.8MW)	0.43±0.32	0.55±0.08	3.3±0.6	1.2±0.1
KJM (2.2 MW)	0.50±0.37	0.58±0.07	2.8±0.5	1.2±0.1

Normalized gradients do not vary significantly, but Te/Ti and ExB shear **do**

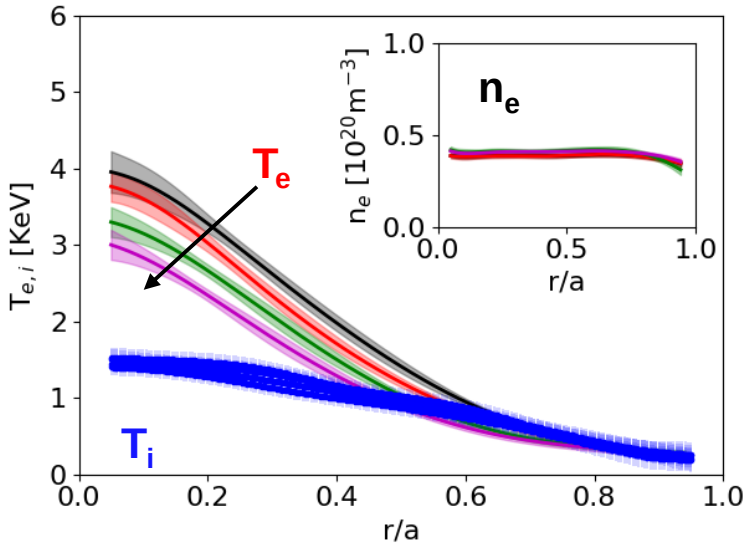

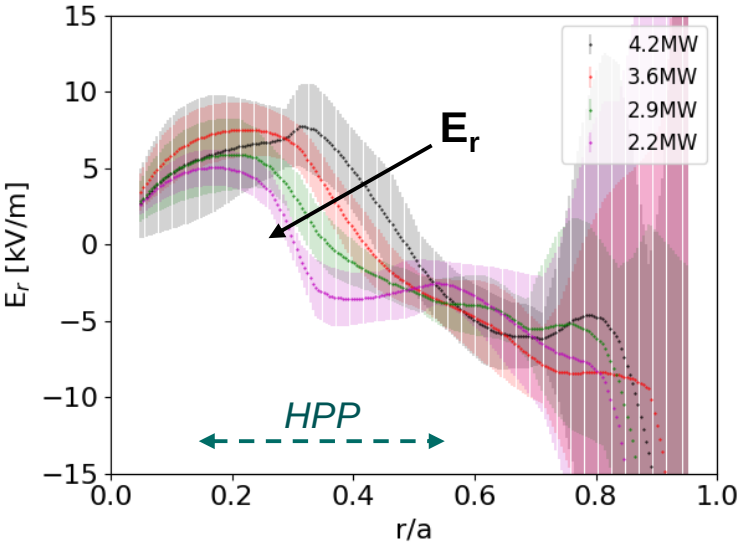

XP:20250508.030

The negative mirror configuration behaves similarly, with a lower achieved gradient → off-axis heating

Er once again varies, with heating power, and the stiffness remains of order 1:

$$n_e\chi_e^{PB} = -q_e/\nabla T_e, \qquad n_e\chi_e^{HP} = -\partial q_e/\partial \nabla T$$

Negative-mirror

(0.2<r/a<0.6)	χ_e^{PB} [m²/s]	χ_e^{HP} [m²/s]	dlnT$_e$/dρ	dlnT$_i$/dρ
XIM (4.3MW)	0.6±0.3	0.7±0.2	2.4±0.2	1.2±0.1
XIM (3.7MW)	0.5±0.3	0.55±0.16	2.7±0.4	1.1±0.1
XIM (2.9MW)	0.4±0.3	0.7±0.2	2.7±0.4	1.2±0.1
XIM (2.2 MW)	0.3±0.2	0.50±0.07	2.6±0.1	1.3±0.1

Normalized gradients do not vary significantly, but Te/Ti and ExB shear **do**

Reduced on-axis magnetic field, 2.486T, is required in Negative mirror → off-axis heating @ r/a~0.2

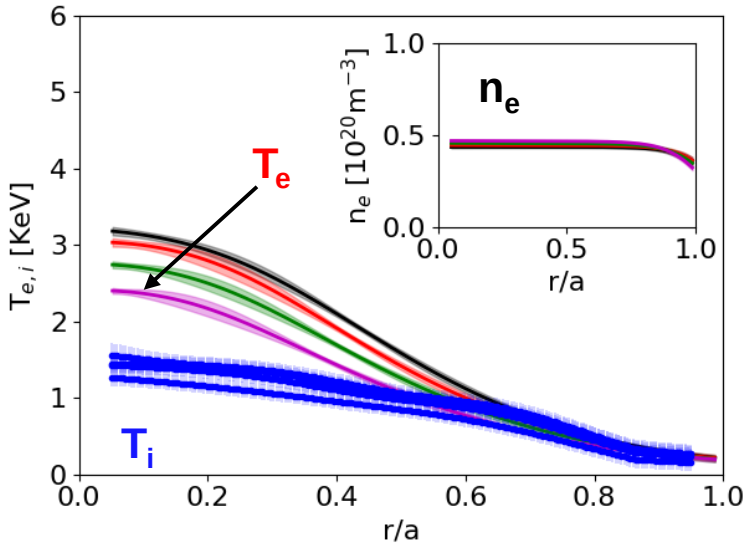

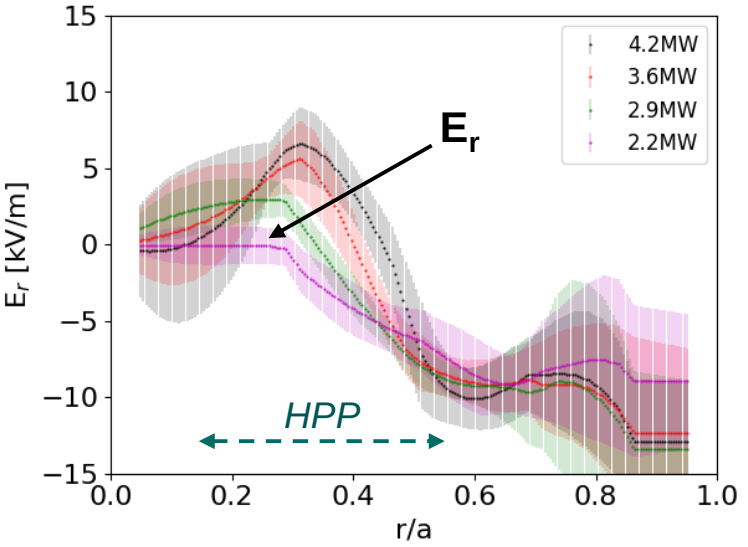

XP:20250507.033

Low-mirror has a significant variation in heat pulse diffusivity

In contrast to High-mirror : Er does not change significantly with power

→ Increased stiffness

$$n_e\chi_e^{PB} = -q_e/\nabla T_e, \qquad n_e\chi_e^{HP} = -\partial q_e/\partial \nabla T$$

Low-mirror

(0.2<r/a<0.6)	χ_e^{PB} [m²/s]	χ_e^{HP} [m²/s]	dlnT$_e$/dρ	dlnT$_i$/dρ
AIM (4.2MW)	0.2±0.2	**1.3±0.2**	3.0±0.5	1.1±0.1
AIM (3.7MW)	0.2±0.2	**1.1±0.1**	3.1±0.6	1.1±0.1
AIM (2.9MW)	0.13±0.2	**0.6±0.2**	3.2±0.6	1.1±0.1
AIM (2.0 MW)	0.14±0.2	**0.46±0.32**	3.1±0.8	1.0±0.1

Normalized gradients do not vary significantly, but Te/Ti does

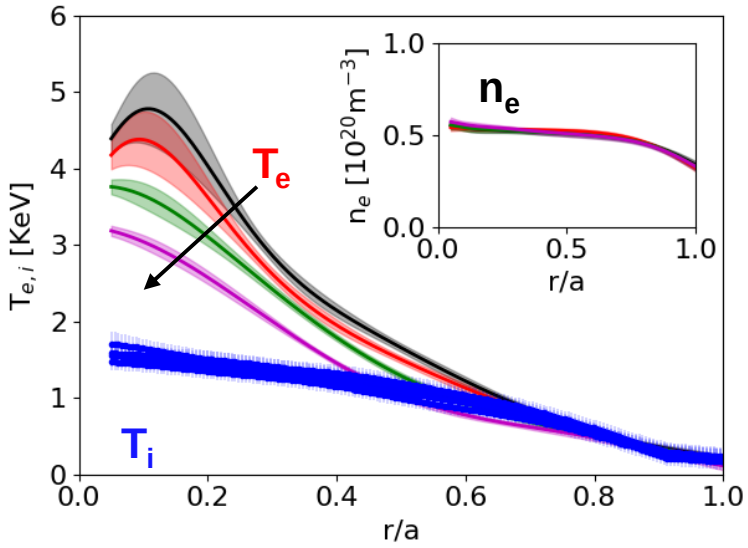

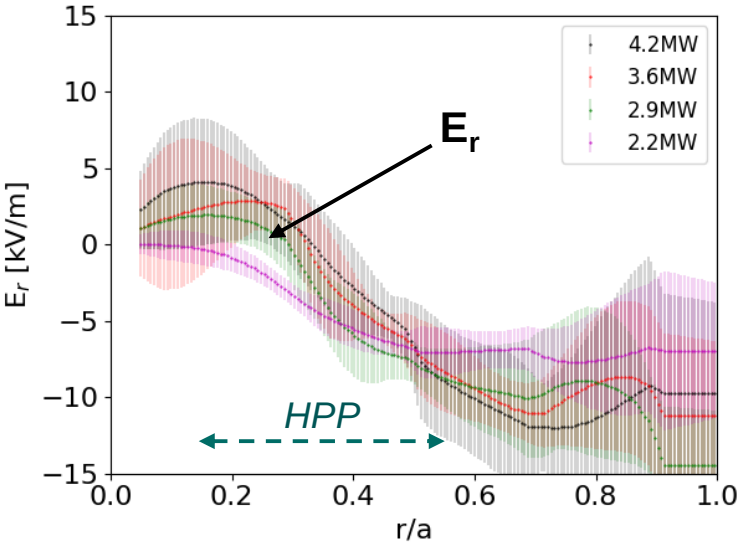

XP:20250429.070/73/79

Low-mirror has a significant variation in heat pulse diffusivity, accompanied by increased core T_e fluctuations

In contrast to High-mirror : Er does not change significantly with power

→ Increased stiffness $0.5<\chi_e^{HP}<1.3$ m²/s

$$n_e\chi_e^{PB} = -q_e/\nabla T_e, \qquad n_e\chi_e^{HP} = -\partial q_e/\partial \nabla T$$

Low-mirror

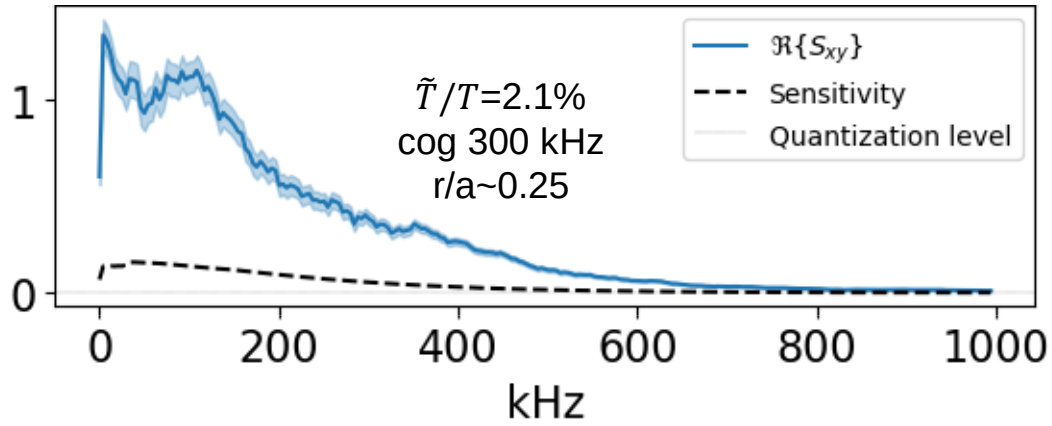

Normalized gradients do not vary significantly, but Te/Ti does

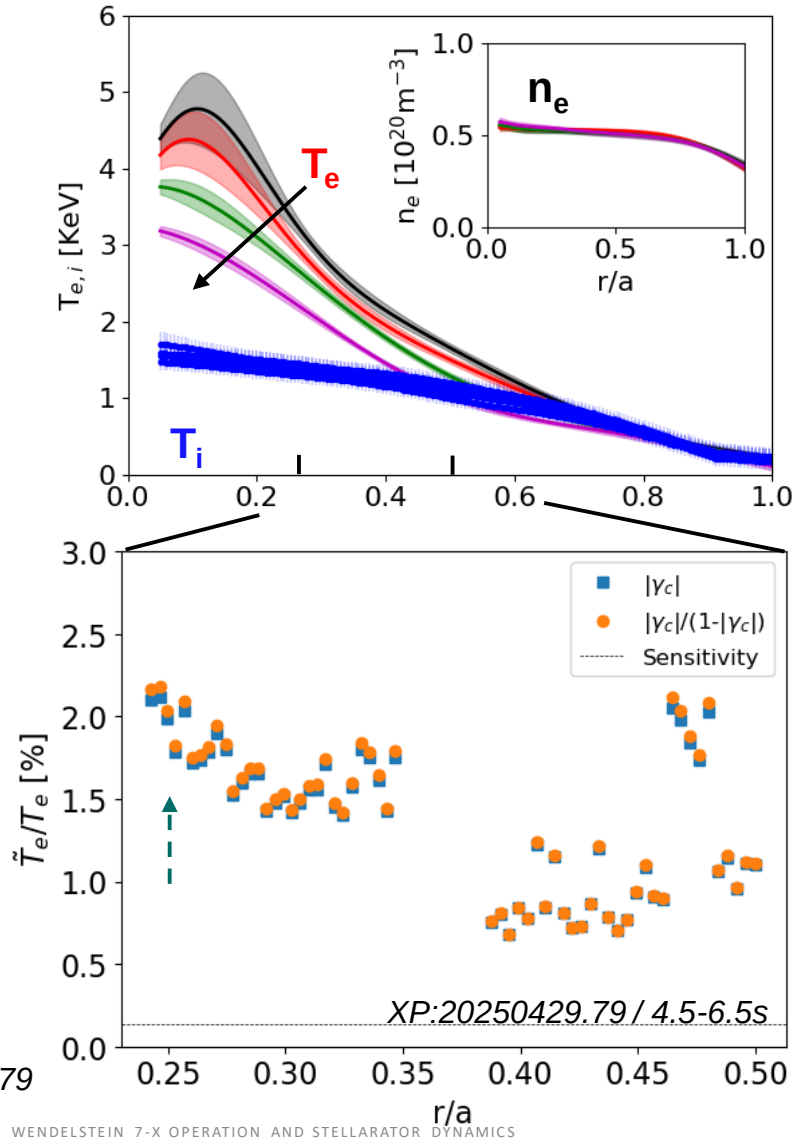

XP:20250429.070/73/79

In the low-iota configuration, the stiffness increases significantly

The electron root region disappears, and the stiffness increases by nearly a factor of 2 in comparison to the High-iota configuration:

$$n_e\chi_e^{PB} = -q_e/\nabla T_e, \qquad n_e\chi_e^{HP} = -\partial q_e/\partial \nabla T$$

Low-iota

(0.2<r/a<0.6)	χ_e^{PB} [m²/s]	χ_e^{HP} [m²/s]	dlnT$_e$/dρ	dlnT$_i$/dρ
DBM (4.4MW)	0.3±0.2	**0.9±0.14**	3.7±0.5	1.2±0.1
DBM (4.0MW)	0.3±0.4	**0.9±0.15**	3.4±1.3	1.2±0.1
DBM (3.2MW)	0.3±0.3	**0.8±0.2**	3.4±1.2	1.2±0.1
DBM (2.2 MW)	0.1±0.2	**0.4±0.1**	3.9±1.1	1.1±0.1

Normalized gradients do not vary significantly, but Te/Ti does, and there is **low**-ExB shear

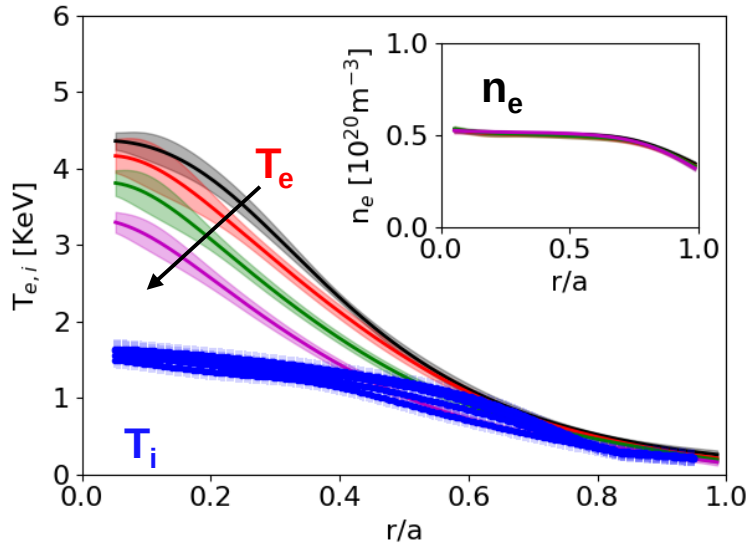

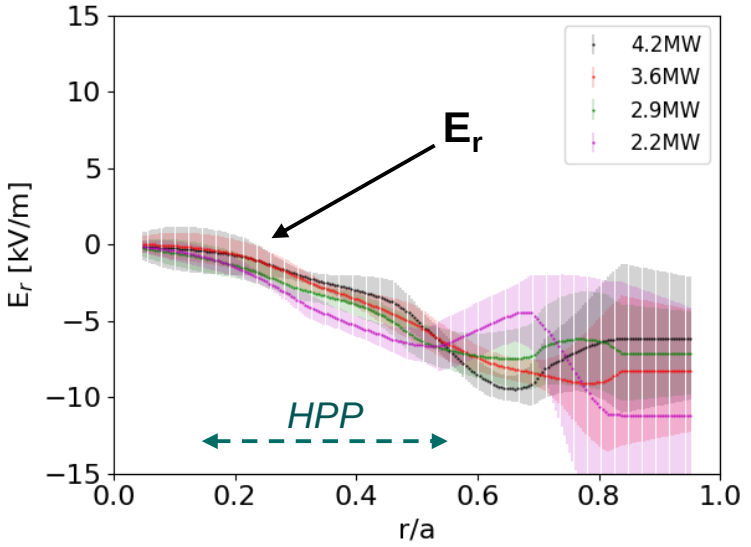

XP:20250401.060

In the low-iota configuration, the stiffness increases significantly, … and core T_e fluctuations increase in same range

The electron root region disappears, and the stiffness increases by nearly a factor of 2 in comparison to the High-iota configuration:

$$n_e\chi_e^{PB} = -q_e/\nabla T_e, \qquad n_e\chi_e^{HP} = -\partial q_e/\partial \nabla T$$

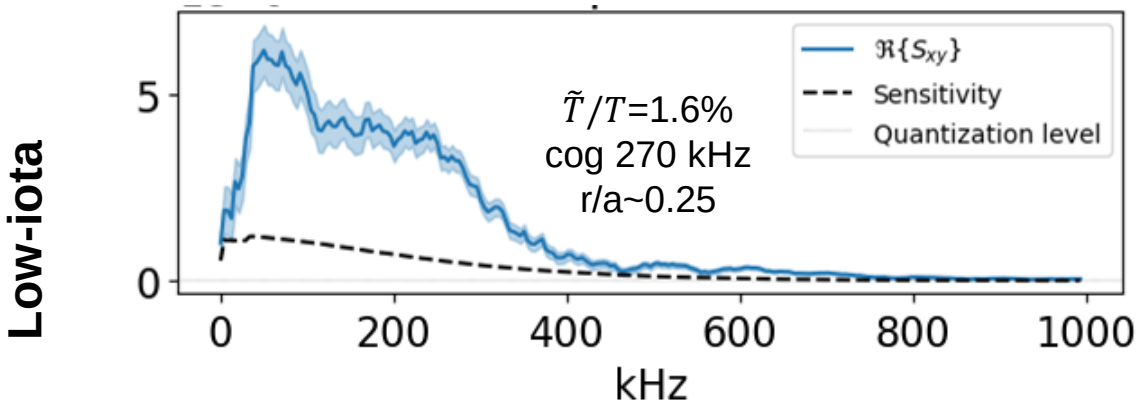

Normalized gradients do not vary significantly, but Te/Ti does, and there is **low**-ExB shear

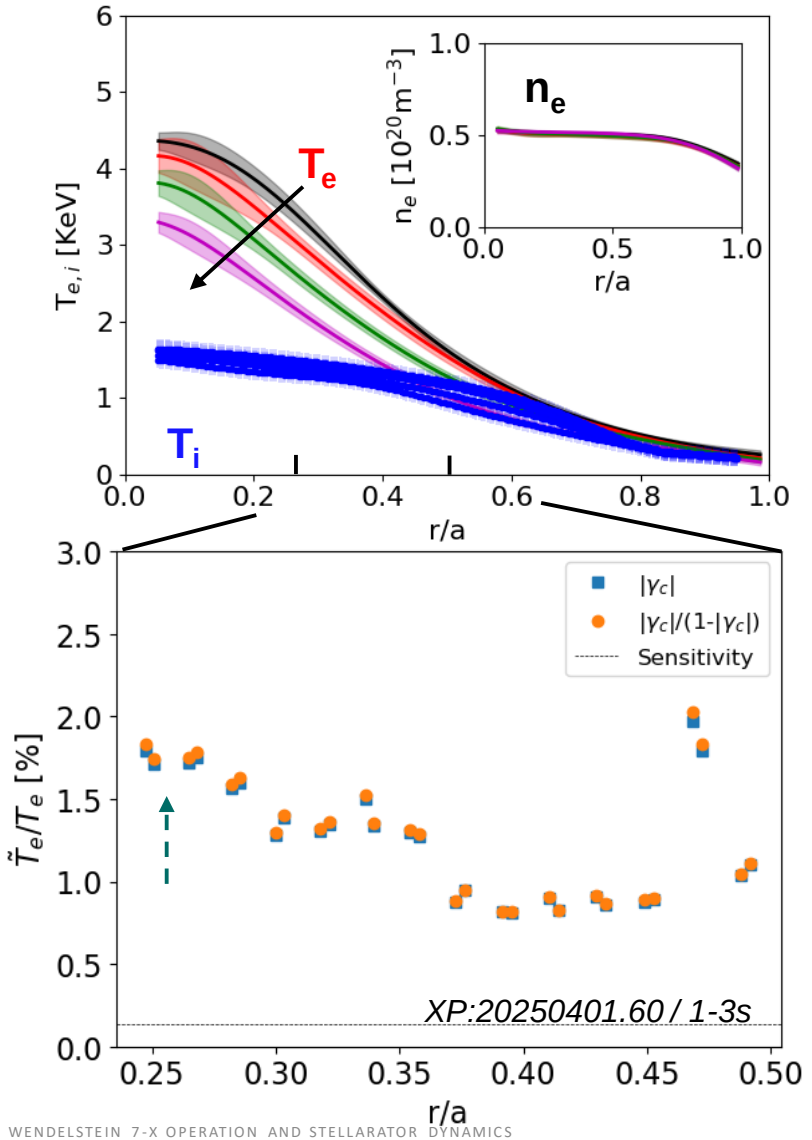

The diffusivities decrease, and stiffness remains low in the High-iota configuration

Heat pulse propagation across the electron-ion root transition region yields a stiffness of the order 1:

$$n_e\chi_e^{PB} = -q_e/\nabla T_e, \qquad n_e\chi_e^{HP} = -\partial q_e/\partial \nabla T$$

High-iota

(0.2<r/a<0.6)	χ_e^{PB} [m²/s]	χ_e^{HP} [m²/s]	dlnT$_e$/dρ	dlnT$_i$/dρ
FTM (4.2MW)	0.3±0.3	0.43±0.06	3.0±0.6	1.2±0.1
FTM (3.8MW)	0.3±0.3	0.40±0.05	3.1±0.6	1.2±0.1
FTM (3.1MW)	0.2±0.2	0.29±0.03	3.1±0.4	1.2±0.1
FTM (2.2 MW)	0.2±0.2	0.40±0.06	3.0±0.3	1.1±0.1

Normalized gradients do not vary significantly, but Te/Ti and ExB shear **do**

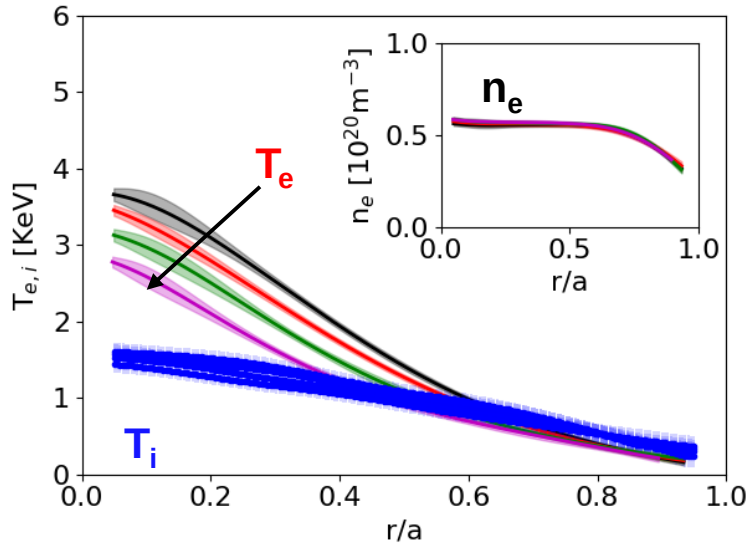

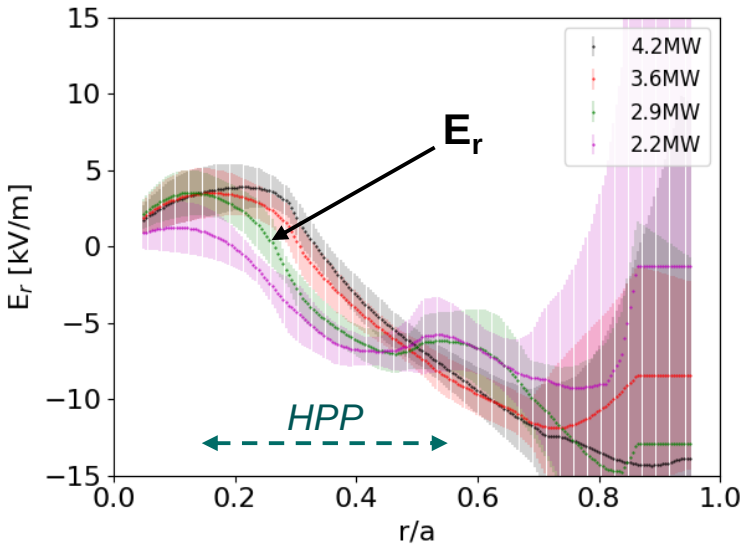

XP:20250429.043

The power balance electron thermal diffusivities remain low in the e-i root transition region,

The heat pulse diffusivities are comparable to low-iota :

$$n_e\chi_e^{PB} = -q_e/\nabla T_e, \qquad n_e\chi_e^{HP} = -\partial q_e/\partial \nabla T$$

Standard

(0.2<r/a<0.6)	χ_e^{PB} [m²/s]	χ_e^{HP} [m²/s]	dlnT$_e$/dρ	dlnT$_i$/dρ
EJM (4.7MW)	0.4±0.3	1.0±0.3	2.6±0.4	1.1±0.1
EJM (4.2MW)	0.2±0.2	0.6±0.1	3.1±0.4	1.2±0.1
EJM (3.8MW)	0.2±0.2	0.6±0.1	3.1±0.5	1.3±0.1
EJM (2.2 MW)	0.1±0.2	0.7±0.2	3.3±0.5	1.3±0.1

Normalized gradients do not vary significantly, but Te/Ti and ExB shear **do**

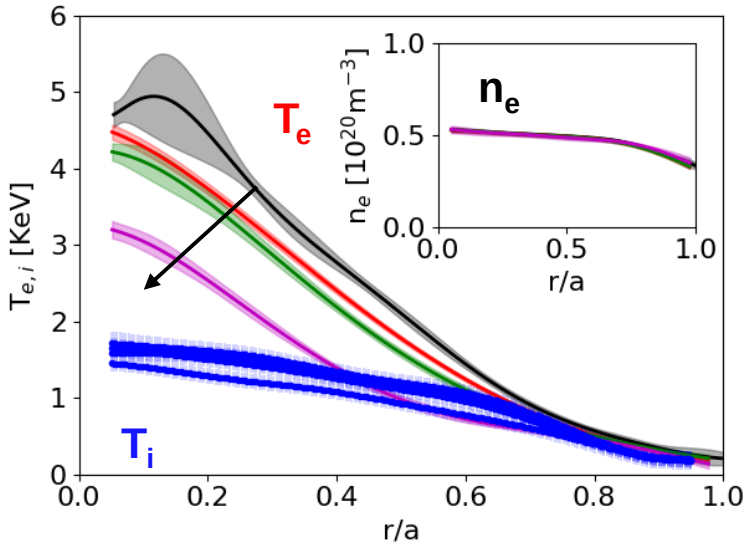

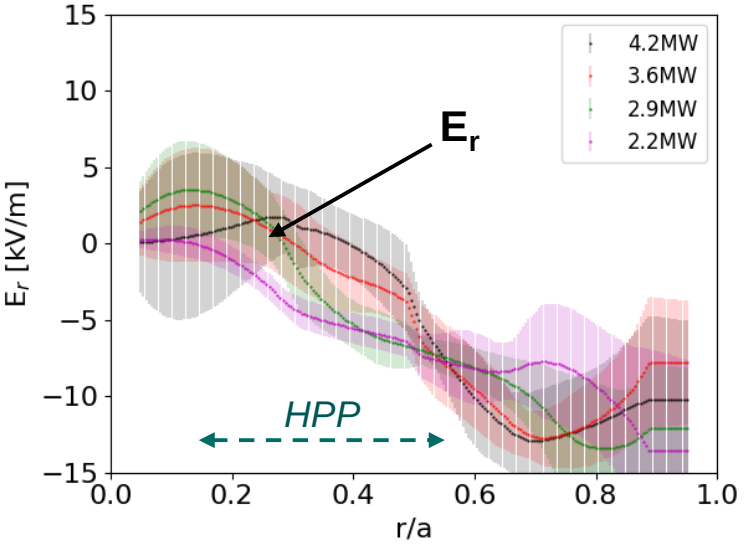

XP:20241210.040/46

There are significiant differences in core energy transport between configurations

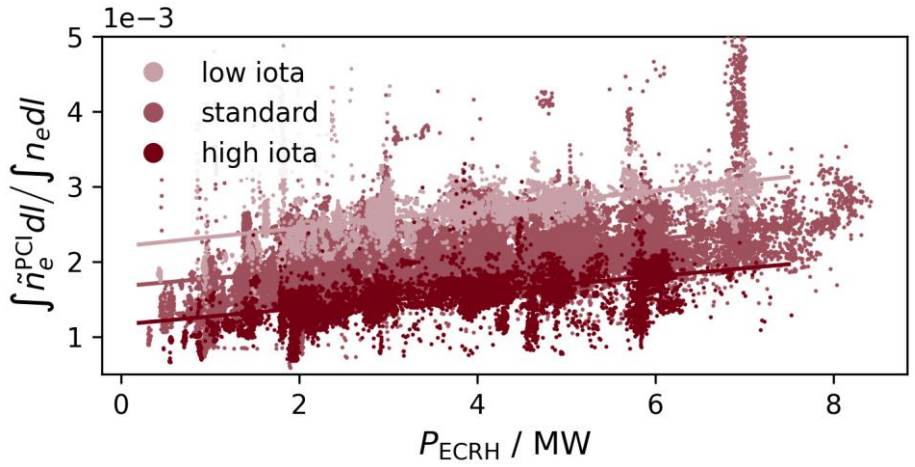

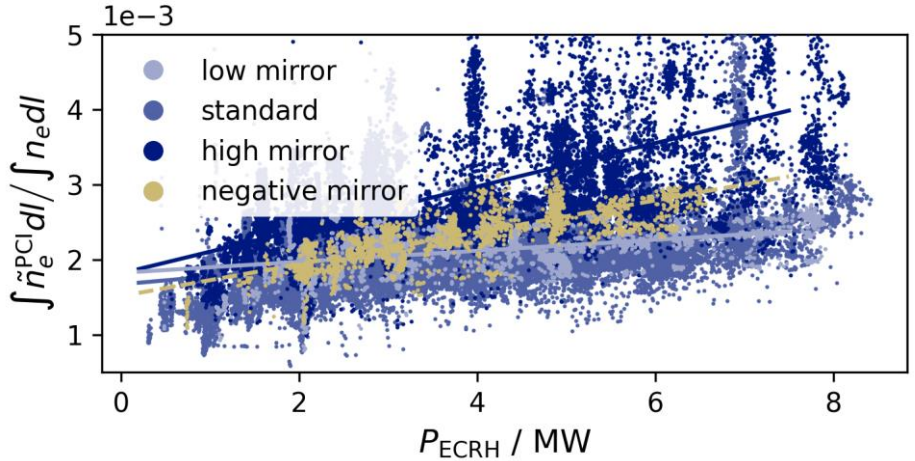

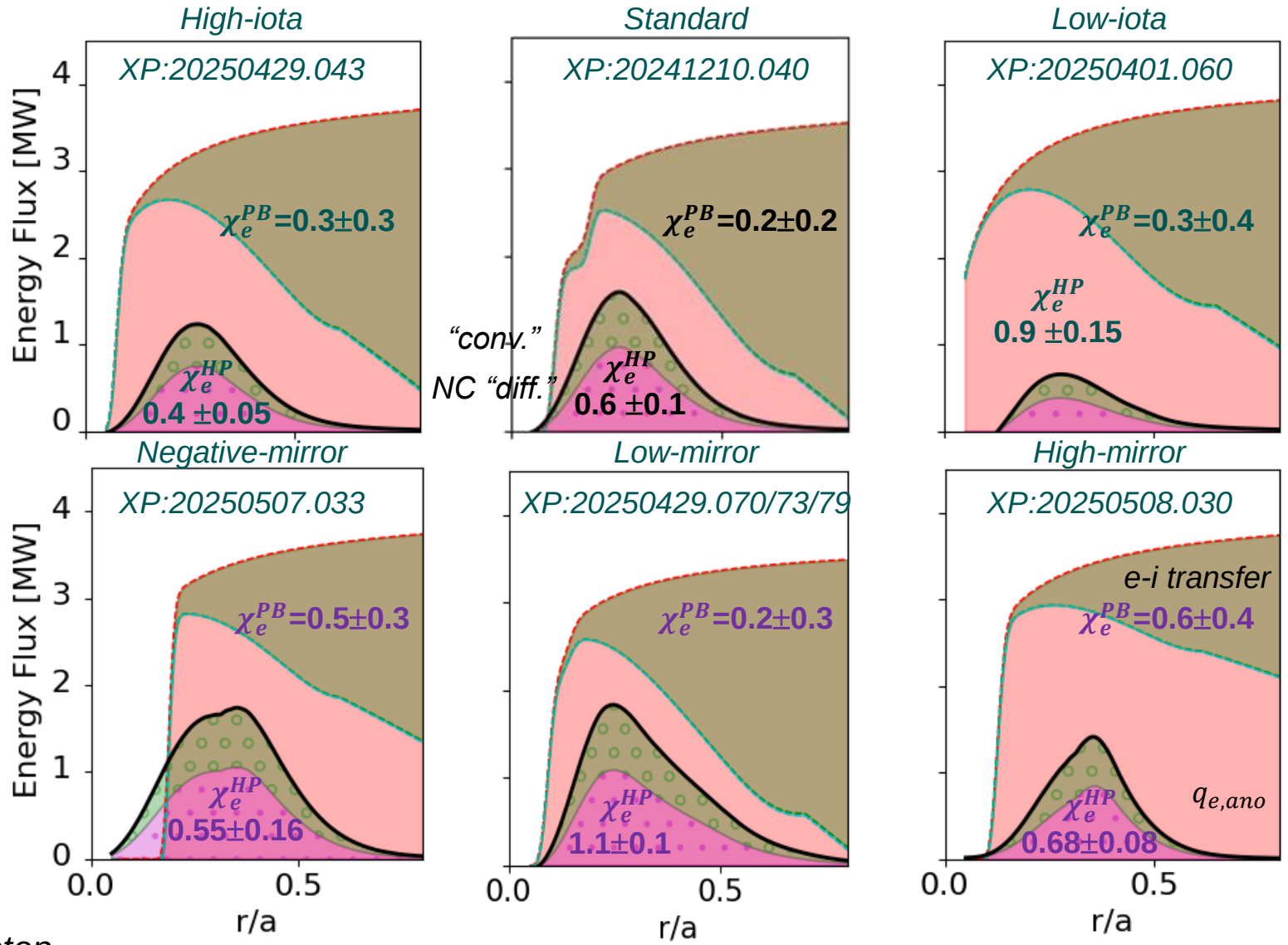

Reported for the common ~3.7 MW heating step

There are significiant differences in core energy transport between configurations

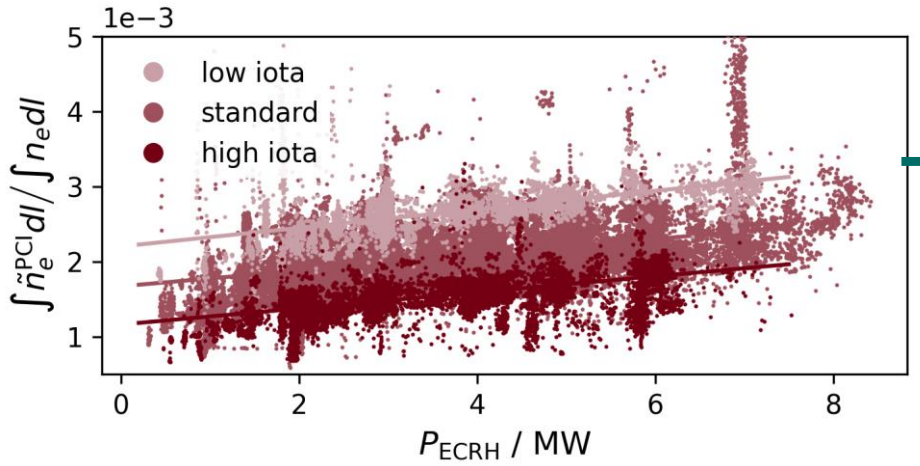

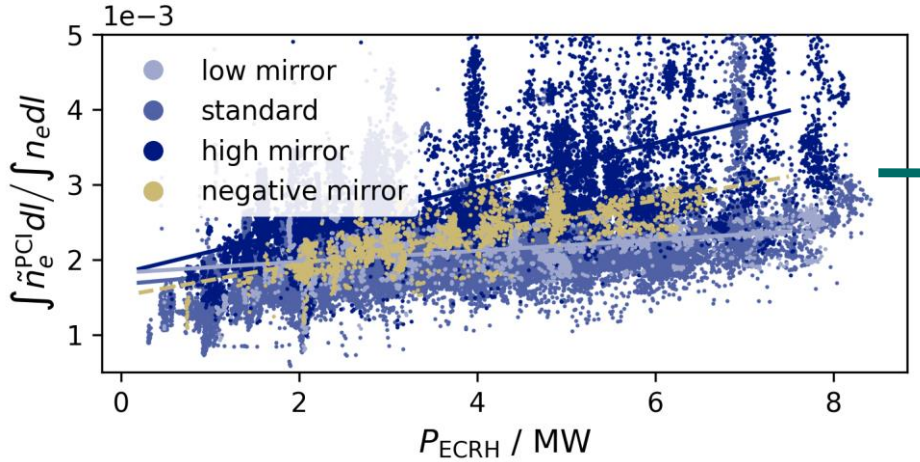

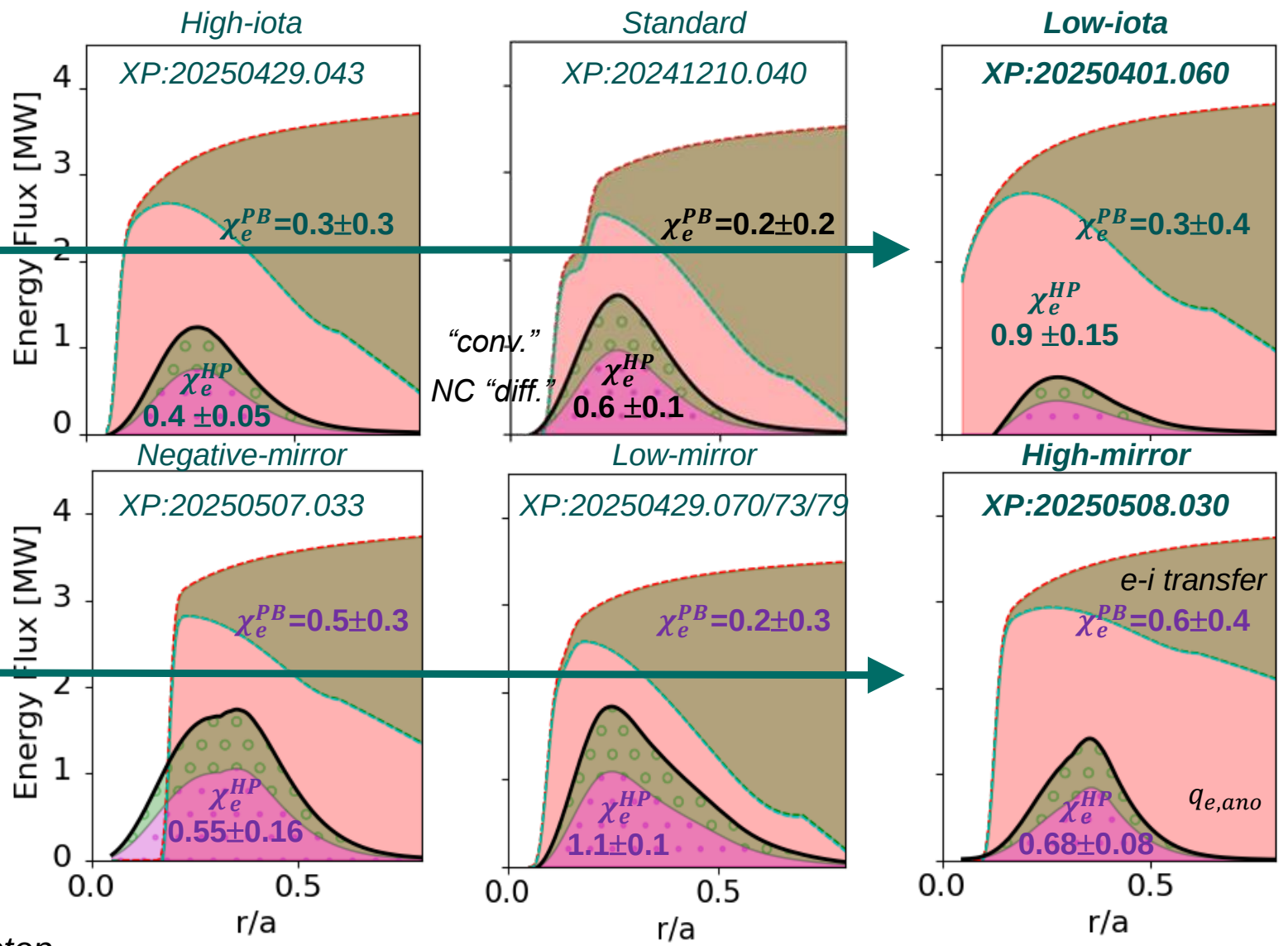

Reported for the common ~3.7 MW heating step

Low-iota and low-mirror configurations have highest χ_e^{HP} and core Te-fluctuations

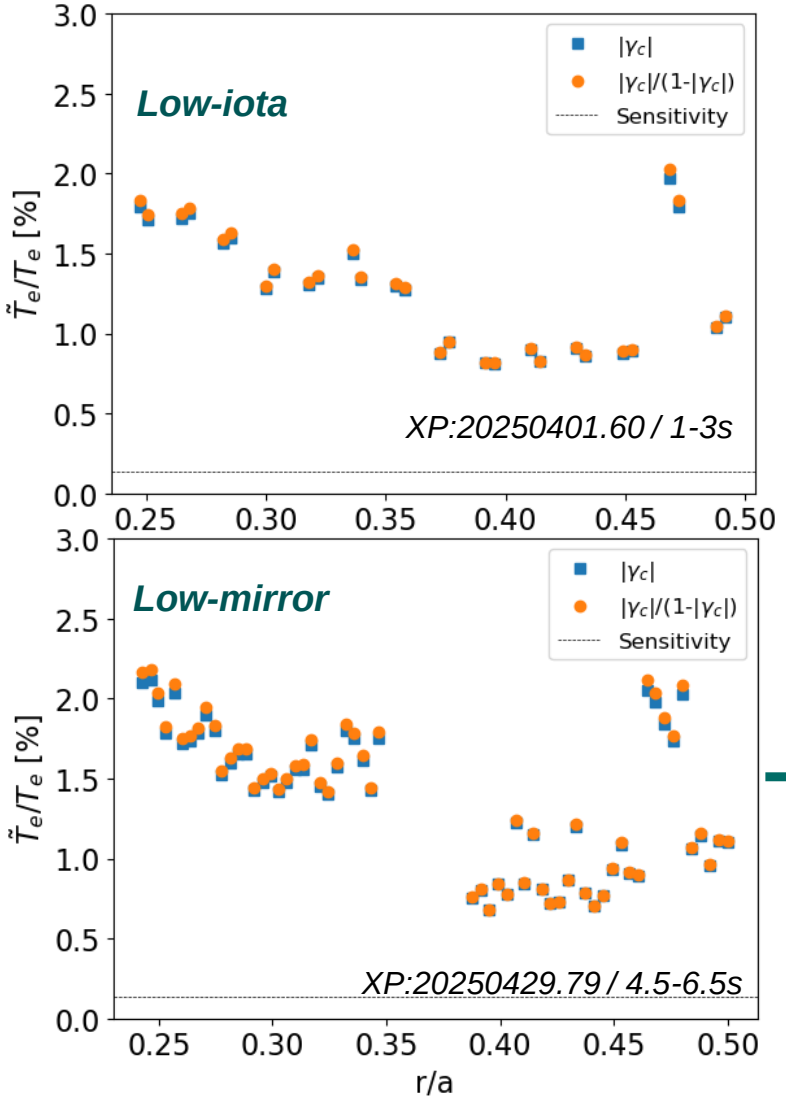

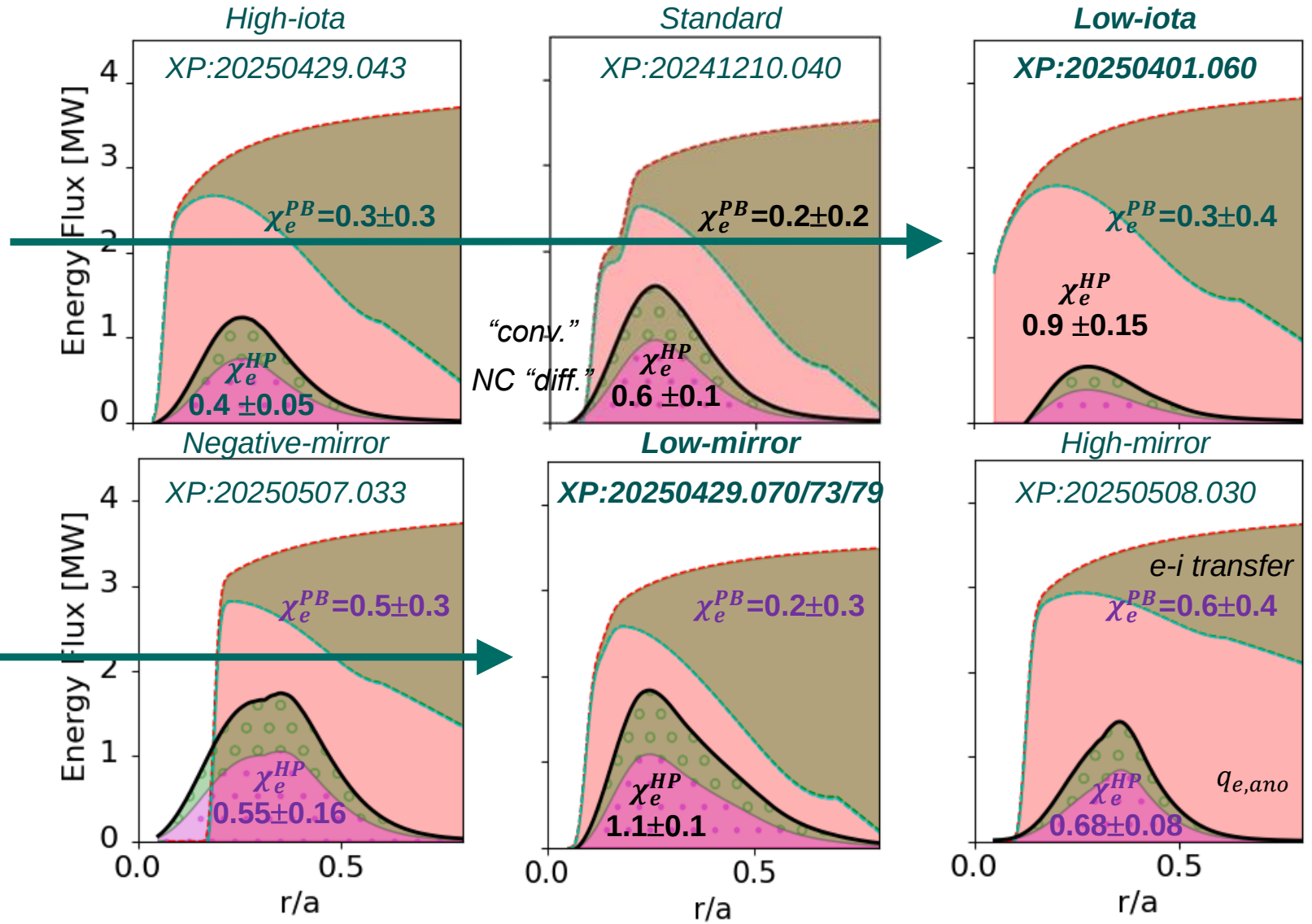

Reported for the common ~3.7 MW heating step

Helium operation is important to W7-X as we prepare for D2 operation (2028+)

- High-mirror: χ_e^{HP} doubles with He at 4MW input
  Negative-mirror: 50% increase
  - **Possible T_e-drive in core?**
- Broadband T_e fluctuations on high-field-side

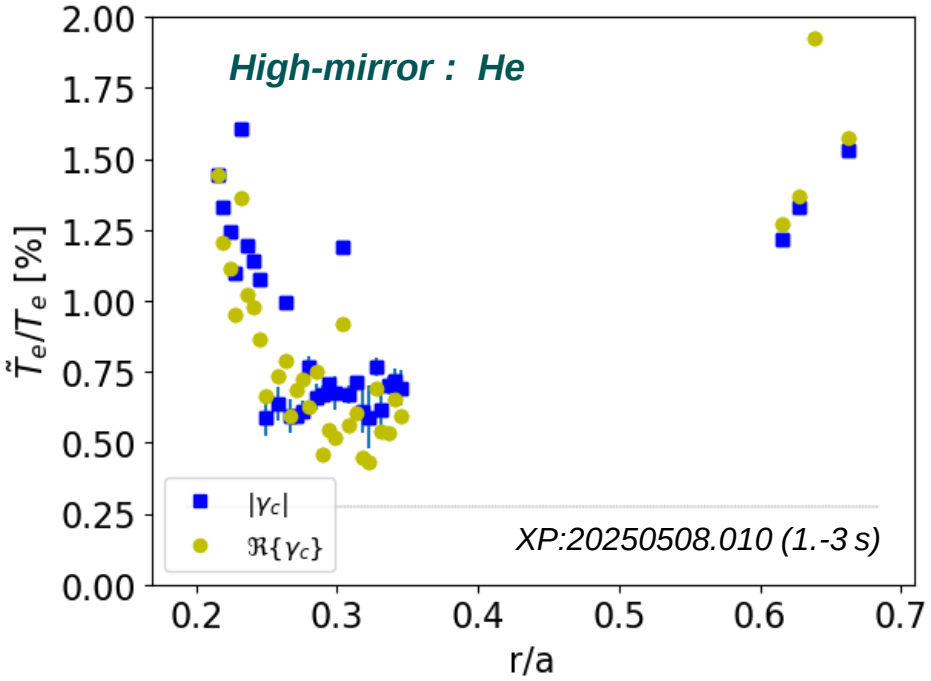

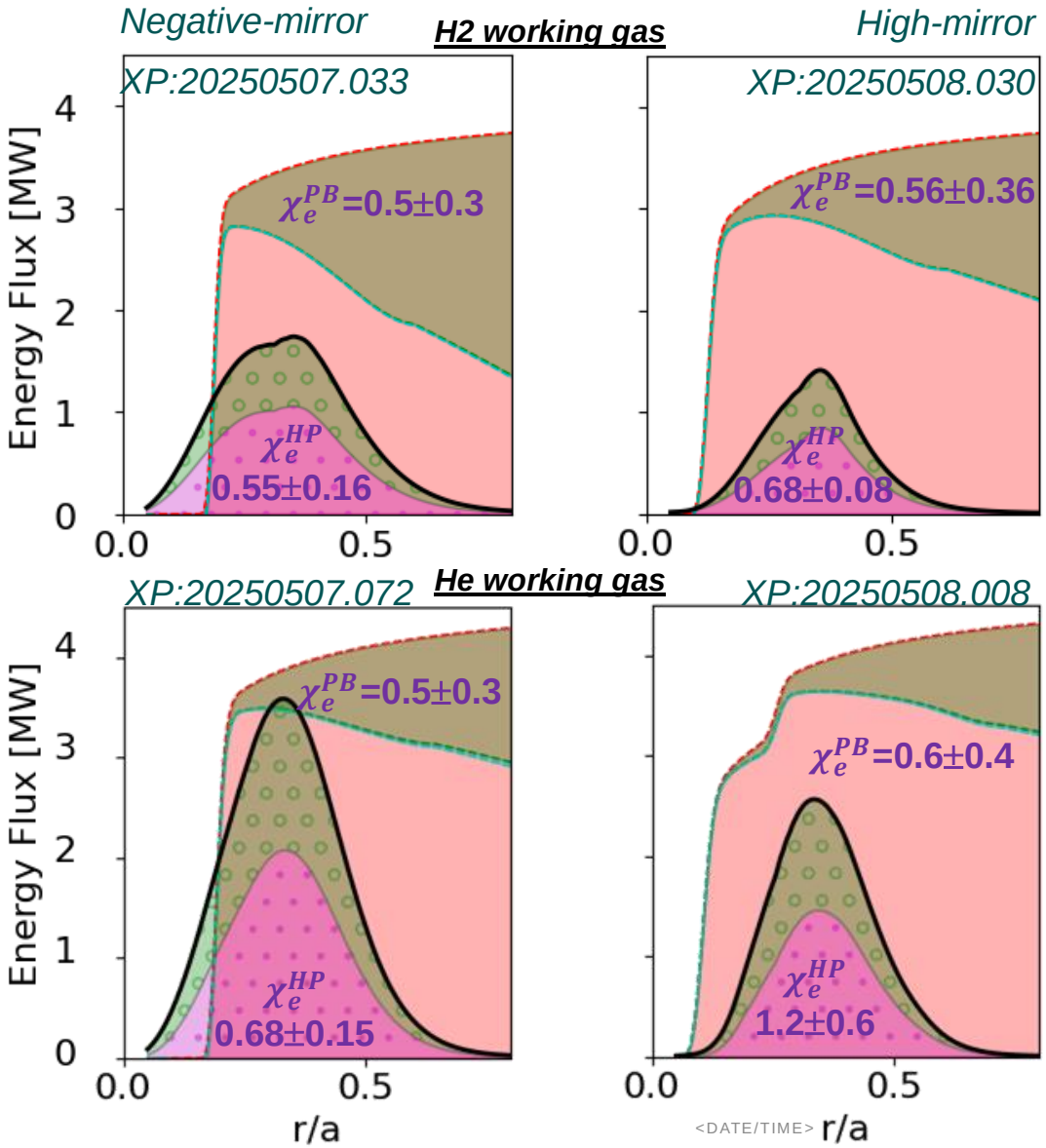

The magnitude of plasma density fluctuations measured by PCI also increase in Helium plasmas

PCI wavenumber-frequency spectra

- diagnostic is “blind” near-zero wavenumber
- positive/negative “k” associated with ExB rotation direction: (forward field)

  k < 0 → outboard-side

  k > 0 → inboard-side

- inboard/outboard asymmetry in high-mirror
- fluctuations increase with …

  … heating power

  … with Helium working gas

High-mirror

Negative Mirror

XP:20250507.033 (1-3/11.5-13.5 s)

H2 working gas

XP:20250508.030 (2-3/12.5-13.5 s)

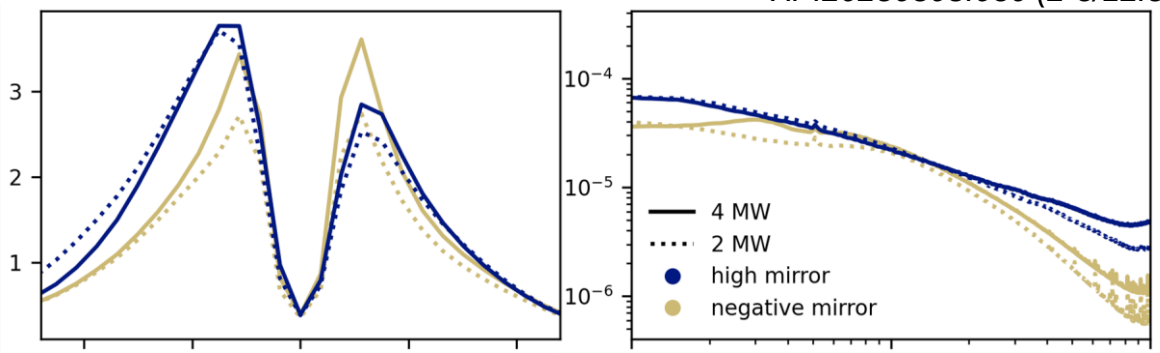

He working gas

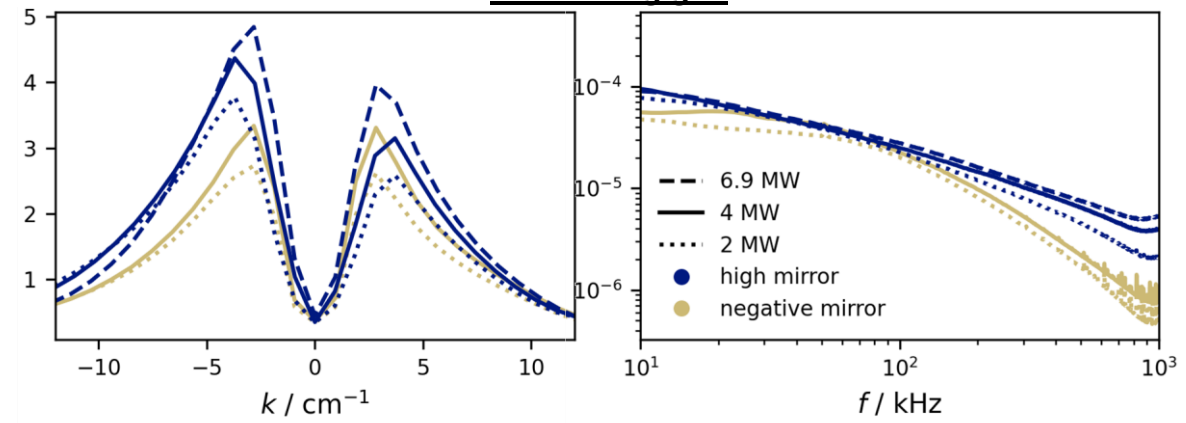

XP:20250507.072 (1-3.5/11.5-14 s)

XP:20250508.010 (1-3/11.5-13.5 s)

Phase velocities in Negative-mirror: fluctuations appear localized to outer half-radius on the outboard side

Phase velocity dominated by single-component

- associated with a local radial electric field
- localizes fluctuations to outer-half radius

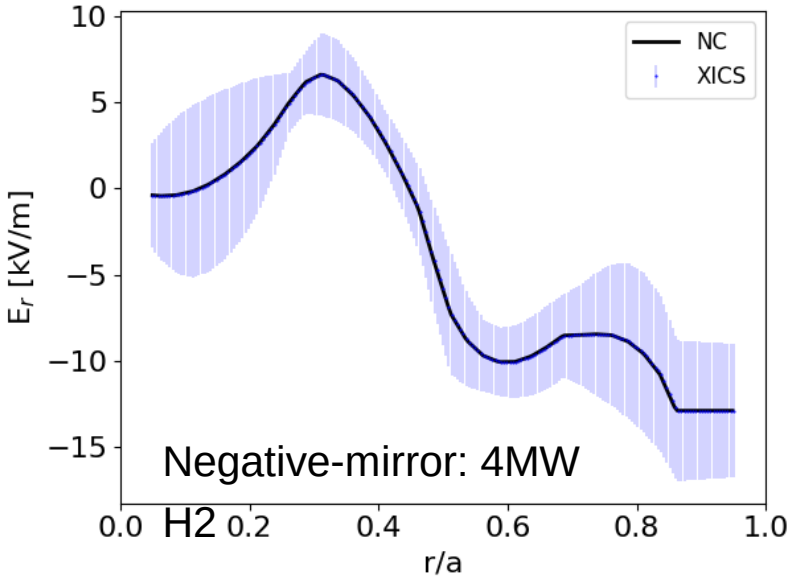

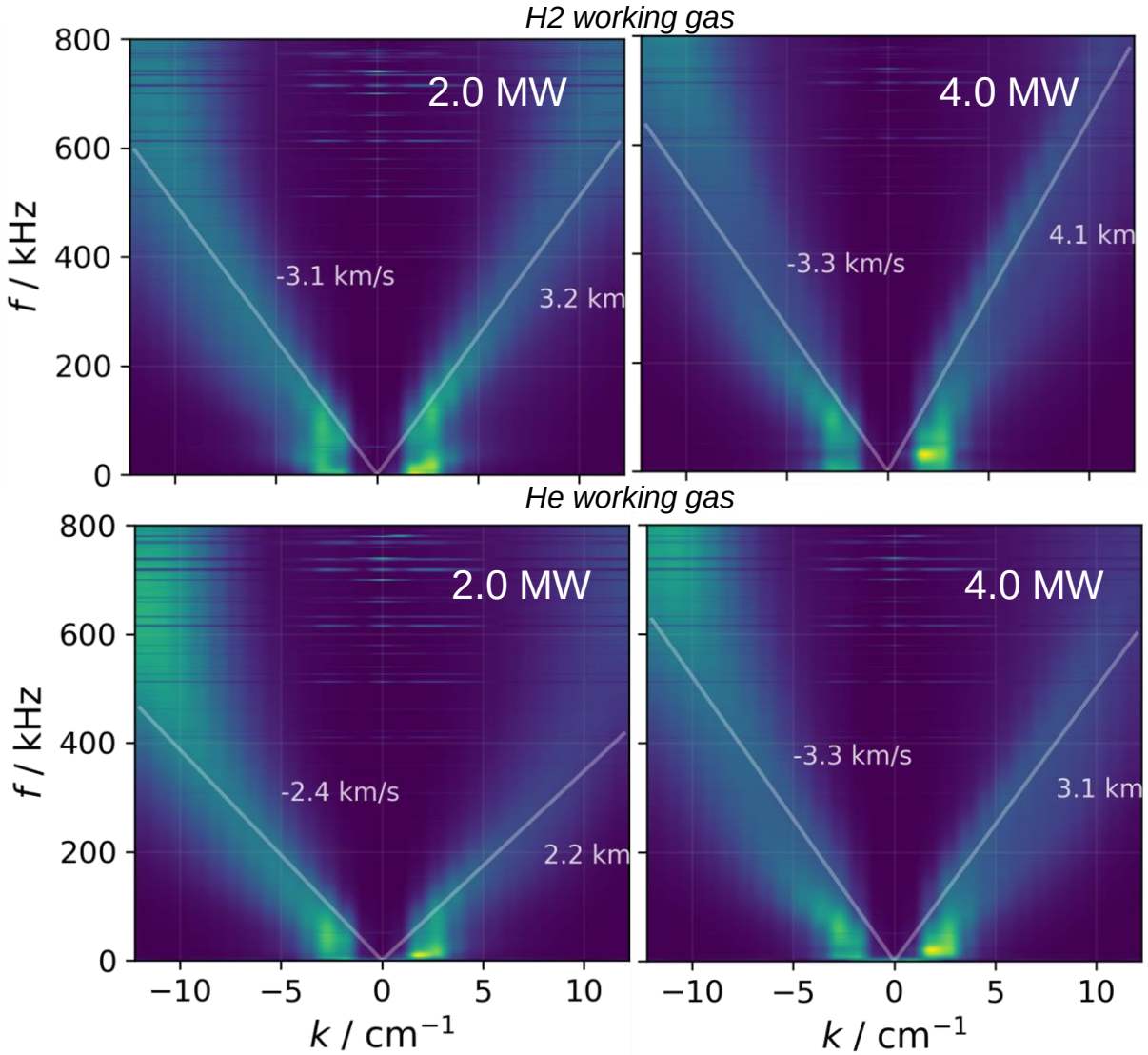

Asymmetry in High-mirror: fluctuations appear localized to outer half-radius on the outboard side

Phase velocity dominated by single-component

- associated with a local radial electric field
- localizes fluctuations to outer-half radius
- increases with heating power

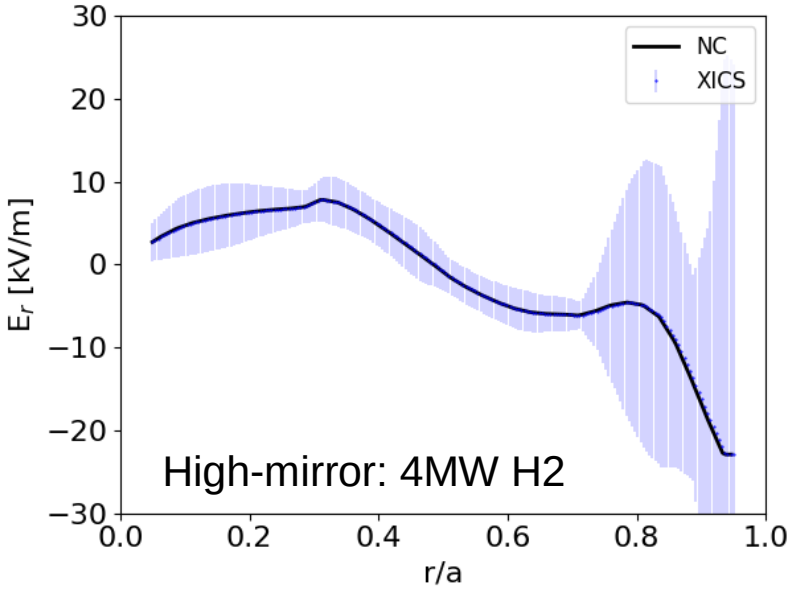

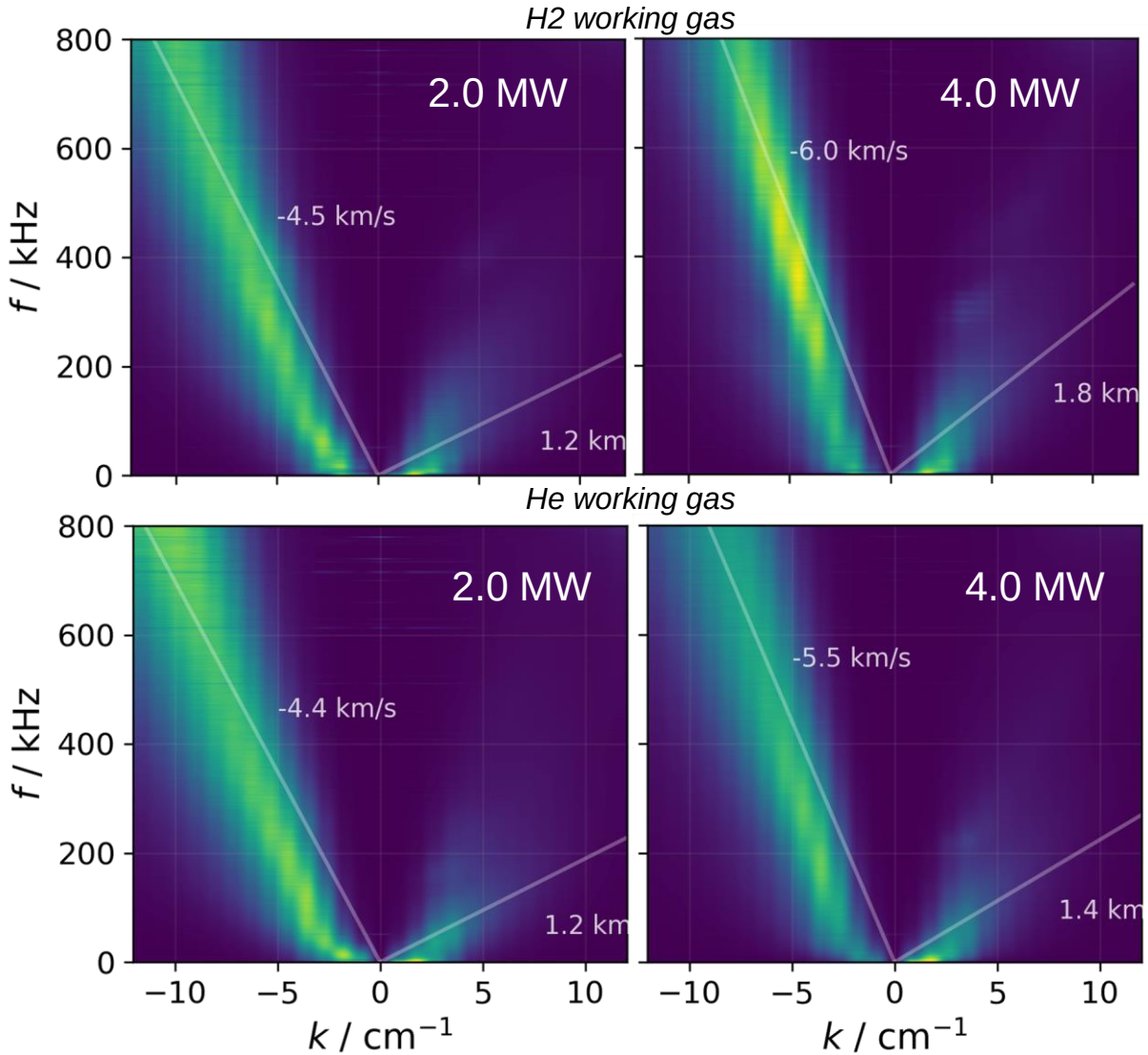

Wendelstein 7-X Contributions at this workshop

Oral and invited talks

C. Killer – Thurs./ 9:00 – Improving plasma confinement by placing magnetic islands inside the LCFS in W7-X

C. Brandt – Fri. / 11:00 – Stability of high beta plasmas in the Wendelstein 7-X stellarator

G. Plunk – Thurs /11:00 – Optimizing the turbulence and confinement of quasi-isodynamic stellarators

D. Carralero – Thurs./12:00 – A multi-machine study on turbulence suppression by density peaking in stellarators

A. Kharwandikar – Thurs./ 9:30 – Empirical scaling of heat transport tin the W7-X Island Divertor

S. Thiede – Wed./9:30 – Analysis of the 3D heat fluxes in the island divertor of W7-X

M. Kriete – Wed./9:00 – How scrape-off layer drift effects change with magnetic field strength in W7-X

R. Davies – Mon. / 12:20 – Fast edge magnetic field optimization techniques and application to Wendelstein 7-X and tokamak-stellarator hybrids

***Posters from our experimental turbulence group*:**

X. Han – P1.26 – *Experimental characterization of a low-frequency coherent oscillation at the plasma edge region of W7-X*

A. Bonciarelli – P2.05 - *Localized probe measurements across magnetic islands: implications for divertor operation in W7-X*

A. v. Stechow – P2.18 – *Reducing core turbulence by gradient control for high performance Wendelstein 7-X plasmas*

T. Windisch – P2.20 – *Doppler backscattering diagnostics at Wendelstein 7-X*

E. Maragkoudakis – P2.21 – *Investigating the impact of the magnetic mirror ratio on the amplitude of density fluctuations and the radial electric field in Wendelstein 7-X*

J.P. Bähner – P2.24 – *Turbulent density fluctuations in Wendelstein 7-X increased iota configurations with internal magnetic islands*

Helium operation is important to W7-X as we prepare for D2 operation (2028+)

- High-mirror: χ_e^{HP} doubles with He at 4MW input
  Negative-mirror: 50% increase
  - **Possible T_e-drive in core?**
- Broadband T_e fluctuations on high-field-side

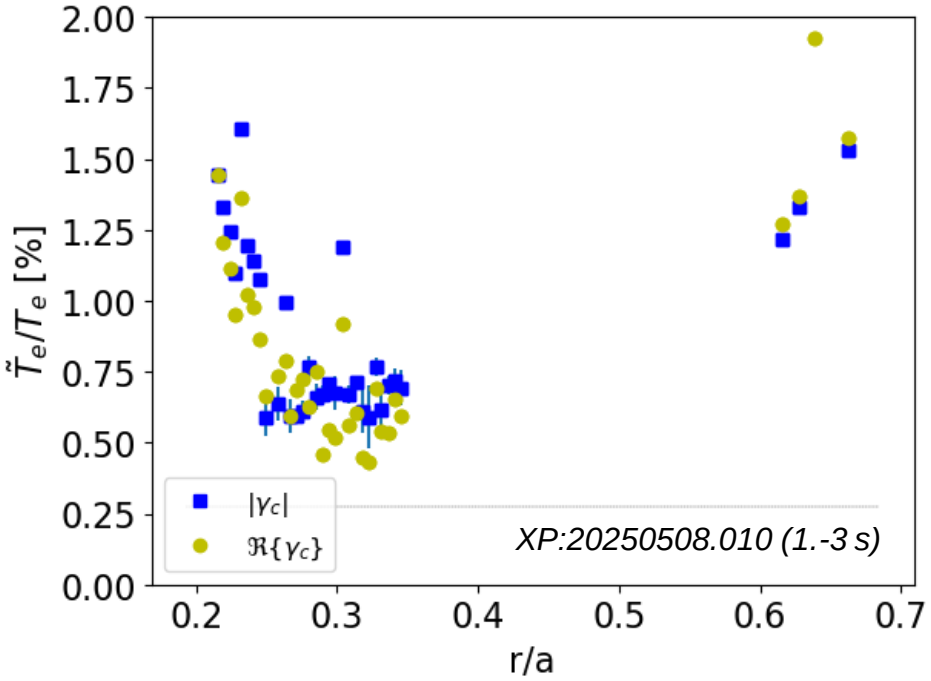

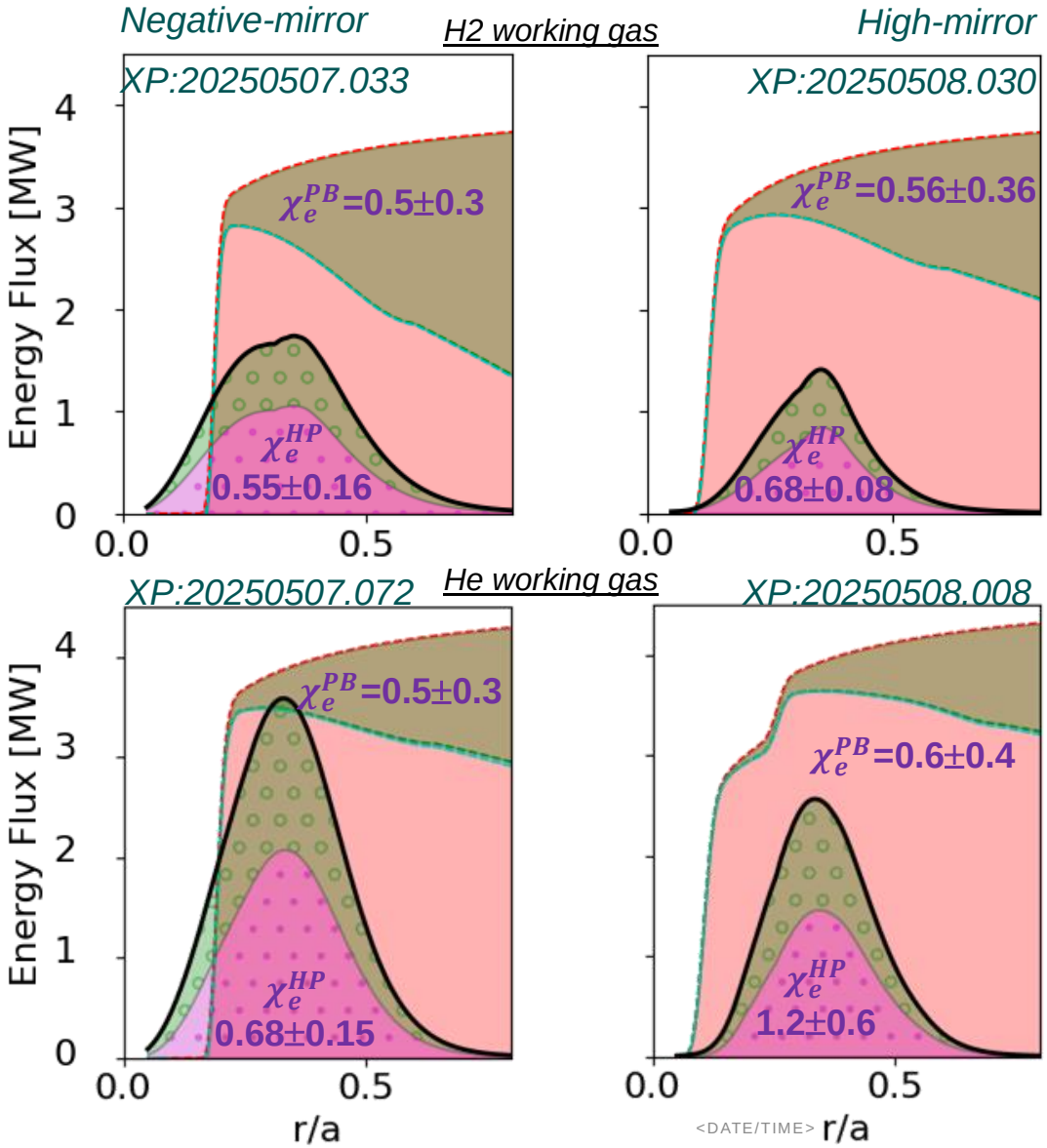

ECE and Thomson: HPP with Helium

XP:20250507.72 /14.0-15.0s

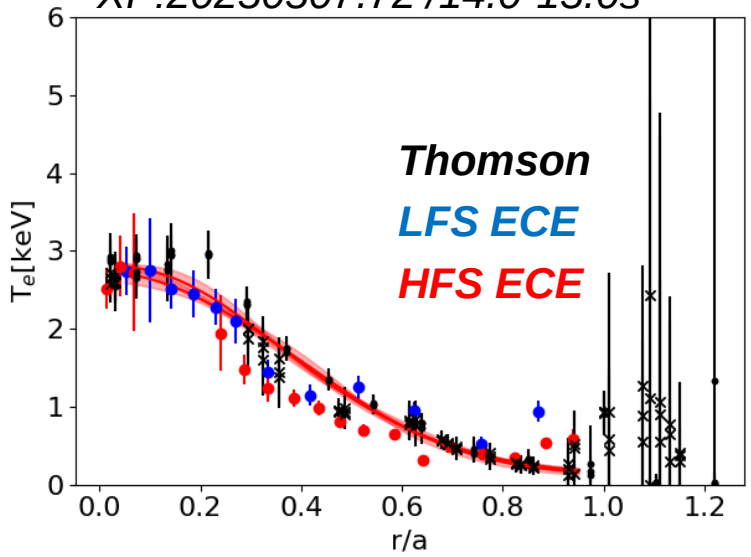

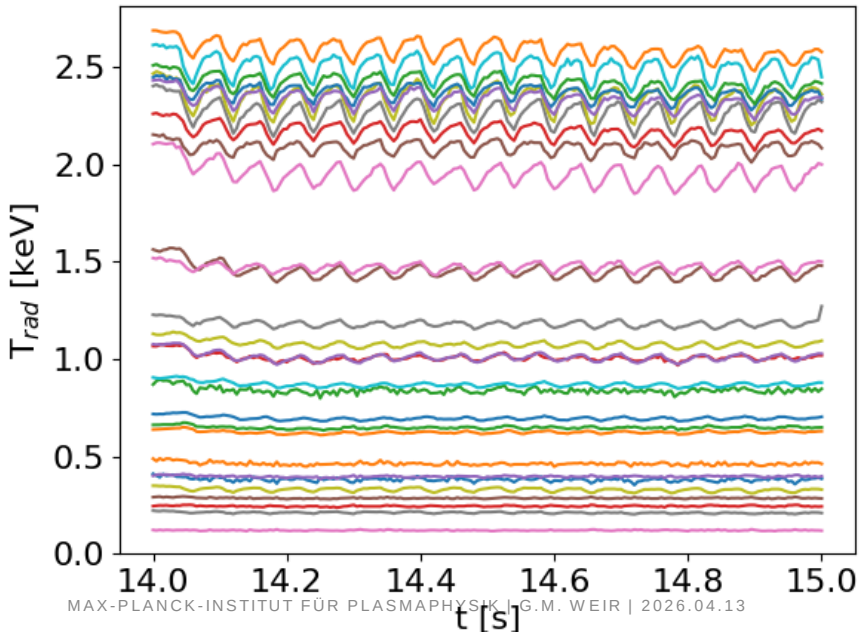

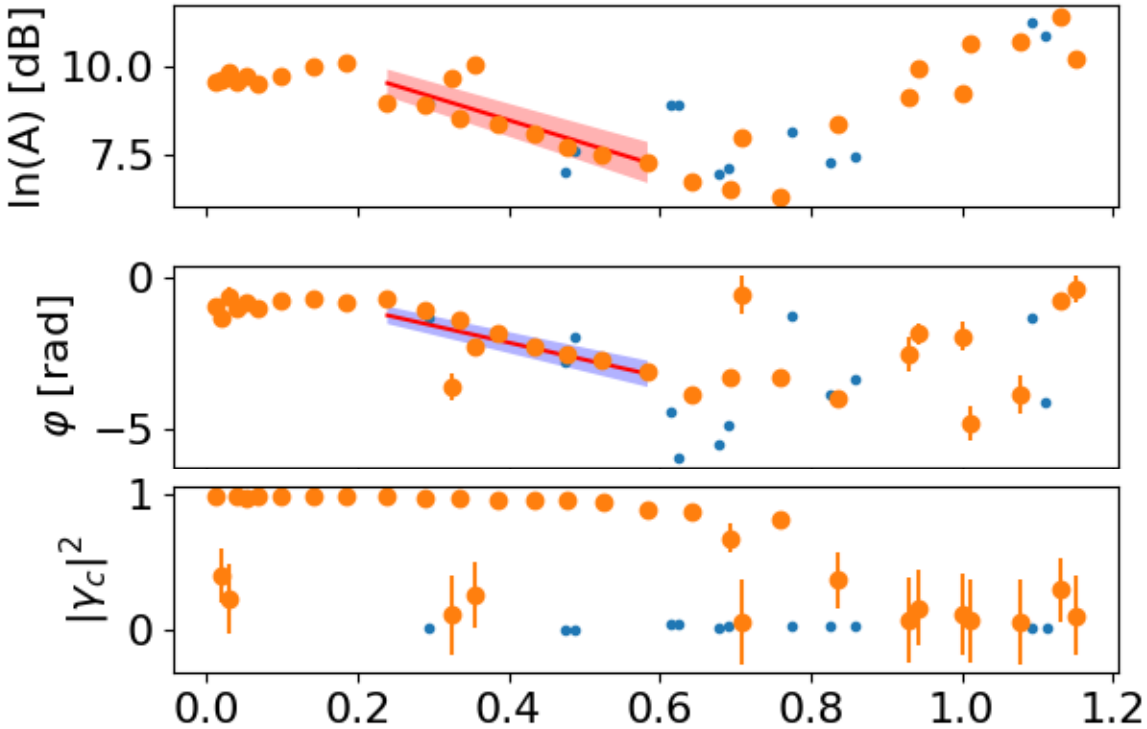

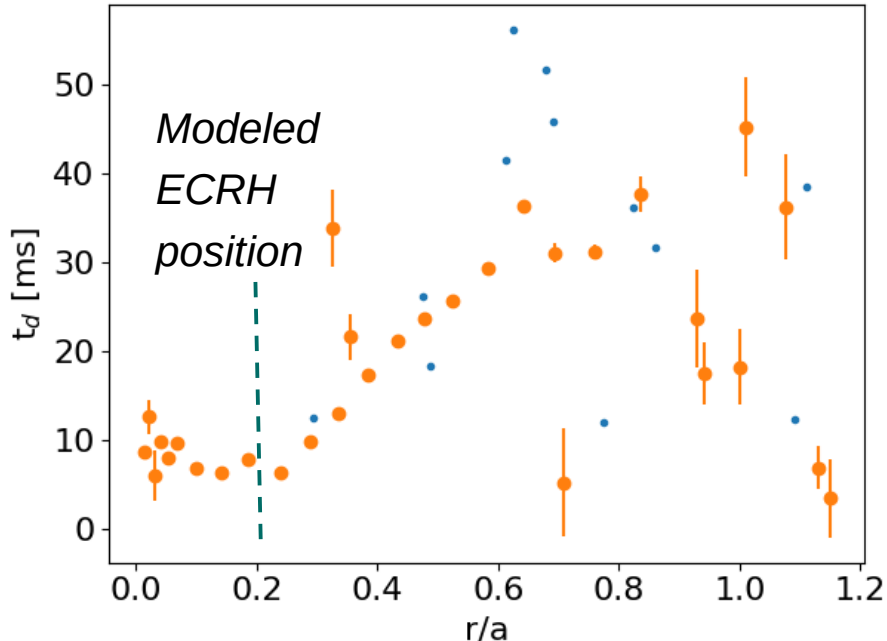

Helium operation is important to W7-X as we prepare for D2 operation (2028+)

- High-mirror: χ_e^{HP} doubles with He at 4MW input
  Negative-mirror: 50% increase
  - **Possible T_e-drive in core?**
- Broadband T_e fluctuations on high-field-side